An In Vitro Analysis of PPARα and CYP4A as Potential Biomarkers for Perfluoroalkyl Acid Exposure in Cetacean Kidney Cells

Kaylee Danae Kautz

A Thesis submitted in partial satisfaction of the requirements
for the degree Master of Science

in

Marine Science

College of Natural and Computational Sciences

Hawai‘i Pacific University

Spring 2019

Honolulu, Hawai‘i

Advisory Committee:

Brenda Jensen, Chair
Jennifer Lynch
Yongli Chen

ABSTRACT

Concern for the high concentration of PFAAs seen in marine mammals has led to the investigation of the effect of these chemicals on their health. Two proteins have been suggested as potential biomarkers for PFAA exposure, peroxisome proliferator-activated receptor alpha (PPARα) and cytochrome P450 4A (CYP4A). PPARα is a transcription factor, which induces transcription of CYP4A, and PFAAs have been documented to activate PPARα in other mammals including mice, humans, and Baikal seals. Additionally, there is a correlation in cetaceans stranded in Hawaii between high concentrations of PFAAs and PPARα mRNA and CYP4A protein expression. We measured protein expression of PPARα and CYP4A in *Tursiops truncatus* kidney cells exposed *in vitro* to four PFAAs, PFOA, PFDA, PFOS, and PFNA. The relative expression of each protein was quantified using Western Blot. At the highest dose (225 uM), all four chemicals induced greater expression of PPARα than the vehicle control, but this increase in expression was not statistically significant ($p < 0.05$). There was a statistically significant difference between the protein expression of PPARα in cells exposed to the two lower concentrations of PFNA (1 uM and 25 uM) and the highest concentration (225 uM) ($p = 0.0288$). All four chemicals elicited a dose dependent response in expression of CYP4A; however, the change in expression was not significantly different between treatment groups and from the vehicle control ($p < 0.05$) with the exception of PFOS. Although we did see a dose-response effect, our results suggest that these two proteins are not ideal biomarkers for PFAA exposure in cetaceans due to the high sensitivity of the pathway in the narrow range of doses tested. However, this does not lessen the concern for how these chemicals are disrupting this pathway in cetaceans, as higher doses induce expression similar to or greater than known

positive controls. This is the first *in vitro* study to investigate the potential of PPARα and CYP4A as biomarkers of PFAAs exposure in cetacean cells.

HAWAI'I PACIFIC UNIVERSITY

An In Vitro Analysis of PPARα and CYP4A as Potential Biomarkers for Perfluoroalkyl Acid Exposure in Cetacean Kidney Cells.

by

Kaylee Danae Kautz

April 18, 2019

This thesis is submitted in partial fulfillment of the requirements for the degree of Master of Science in Marine Science at Hawai'i Pacific University. We the undersigned have examined this document and have found that it is complete and satisfactory in all respects, and all revisions required by the final examining committee have been made.

Author _____

Kaylee D. Kautz

Committee Chair _____

Brenda Jensen, Ph.D.

Committee Member _____

Jennifer Lynch, Ph.D.

Committee Member _____

Yongli Chen, Ph.D.

Dean _____

Brenda Jensen, Ph.D., Dean, College of Natural and Computational Sciences

Acknowledgements

I would like to thank Dr. Brenda Jensen for her time and dedication as my Advisor. Her encouragement and guidance through this project were invaluable. I am so thankful for her help through the last few months of my project, which were a very trying time for me, and for her support and enthusiasm in helping me complete my degree. I would like to thank Jennette VanderJagt for starting this project, and letting me continue on with her initial design. I would also like to thank her for teaching me about cell culture technique and her help with the cell dosing process.

I would like to thank the National Institute of Standards and Technology for funding this project, and for contributing to the advancement of my scientific career. Specifically, I would like to thank Jennifer Lynch, who served on my committee and was a wonderful mentor and colleague. Her willingness to set aside a large amount of time to help with calculations and developing my methods was essential to my success. Her dedication as a scientist and mentor will forever inspire me. I would like to thank my two colleagues Melissa Jung and Julia Smith for their encouragement and assistance in the lab.

Additionally, I would like to thank the faculty of Hawai'i Pacific University. I would like to thank Dr. Yongli Chen for the use of her lab space, her assistance in the lab, and her help as a committee member. Specifically, I would like to thank Dr. David Field for his help with writing and Dr. David Hyrenbach for his help with statistics.

Finally I would like to thank my friends and family for their assistance through this process. I could not have succeeded without their support. Specifically I would like to thank my Grandparents for all that they have done to provide me with the best education throughout the

years. I would like to thank my parents for their love, generous help, and continuous support. I would like to thank Jayson for going on this adventure with me in Hawaii and supporting me on my career path.

Table of Contents:

List of Figures:

List of Tables:

CHAPTER 1:

Perfluoroalkyl Acid Exposure in Cetaceans and Links to the PPARα-CYP4A Pathway

Statement of the Problem

High concentrations of PFAAs have been documented in marine mammal tissues around the world (Houde et al., 2011), and there is an increasing concern for potential negative consequences on marine mammal health because of the known effects of exposure in other mammals. The Environmental Protection Agency began investigating concerns about the toxicity, the bioaccumulation, and the persistence of perfluoroalkyl acids (PFAAs) as early as the late 1990's. These concerns grew out of the discovery that PFAAs were accumulating in the tissues of the general human population. Even with increasing regulation to limit exposure in humans and mounting investigation into the environmental impacts of PFAAs, their effect on most marine organisms is still not known. Specifically, there is very little information about the effect of PFAA exposure on marine mammal health.

PFAA exposure has been shown to cause liver, testicular and pancreatic tumors, reproductive and developmental deficits, immunotoxicity, and neurotoxicity in rats and other mammals (Corsini et al., 2014). A study conducted by Kannan et al. (2006) demonstrated that there is a correlation between infectious disease and PFAA concentration in sea otter tissues; however, the effects of exposure have not been adequately investigated at a cellular level in marine mammals. Two studies have linked the PPARα-CYP4A pathway with PFAA exposure in marine mammals (Ishibashi et al., 2004 and Kurtz et al., 2019). These two studies also concluded that this cellular pathway might be useful as a biomarker to monitor exposure to PFAAs in marine mammals. The development of specific biomarkers would be an effective way to elucidate links between exposure levels and toxic effects on a cellular level.

Cellular biomarkers are molecules within the cellular pathway that can be used to indicate exposure to specific toxicants. While many studies quantify the concentration of PFAAs

in cetacean tissues, biomarkers could be a more effective way of monitoring cetacean health. Biomarkers can not only be used to indicate exposure levels in the field, but also directly link toxic effects with specific disrupted cellular pathways. This study will examine two proteins, PPARα and CYP4A, for their potential as biomarkers of perfluoroalkyl acid exposure levels in bottlenose dolphins (*Tursiops truncatus*).

Background

Perfluoroalkyl acids

PFAAs are used in the manufacturing of a wide variety of products. These products include textiles, fabrics, paper, packaging, firefighting materials, mining surfactants, cleaners and pesticides (Rayne and Forest 2009). Their chemical structure makes them ideal repellents for water, grease, and soil (Fair et al., 2012). The wide spread use of PFAAs in manufacturing makes these compounds a concern for both human and ecological health (Fair et al., 2012).

In addition to their ubiquitous use in manufactured goods, the structure and physiochemical properties of PFAAs leads to their continued persistence in the marine environment (Rayne and Forest, 2009). PFAAs have long carbon chains with strong carbon-fluorine bonds (Rayne and Forest, 2009). Carbon-fluorine bonds are much stronger than carbon-hydrogen bonds, and stronger bonds make these compounds highly resistant to degradation (Rayne and Forest, 2009). Lau et al. (2007) describes these compounds as "practically non-biodegradable." Additionally, PFAAs can be both hydrophobic and oleophobic depending on their functional group (Rayne and Forest 2009), meaning that different parts of the molecule repel water and oil, respectively. These properties present a problem for marine environments,

because the molecules can associate with the water and with proteins, which allows for bioaccumulation in organisms (Condor et al., 2007).

PFAAs can be separated into different classes. Two commonly tested classes are perfluoroalkyl sulfonic acids, PFSAs, and perfluoroalkyl carboxylic acids, PFCAs. These compounds contain a hydrophilic acid group that is bonded to the long carbon-fluorine chain (Rayne and Forest 2009). PFAAs have a wide range of chain lengths and branching patterns (Rayne and Forest 2009). The variation in molecular structure is a result of the production process, which produces fluorinated molecules of different chain lengths and different isomers (Lau et al., 2007). The different isomers introduce an obstacle for scientific study, because PFAAs cannot be studied as single component technical products (Rayne and Forest 2009).

The difficulty identifying all of the different PFAA congeners severely limits the understanding of PFAA toxicology as demonstrated by Rayne and Forest (2009). The authors conclude that the current method of quantifying these products by calculating concentrations of only single congener equivalents leaves up to 60-90% of the organofluorine mass in natural waters unidentified. Only the dominant congeners, straight chain isomers, are analyzed in current studies (Rayne and Forest 2009). The difference between calculated concentrations of straight chain isomers and potential concentration of total isomers produced has large implications for the evaluation of toxic load. Considering that all of the chemical isomers cannot be accounted for in current studies, the toxic body burden in marine mammals may be highly underrepresented.

The different PFAAs referred to in this paper are represented by their chemical abbreviations and include: PFOA, PFNA, PFDA, PFUA, PFDoA, PFOSA, PFHxS, PFTA, and PFOS. These are the most common and abundant compounds that are typically measured. Additionally, PFAAs are referred to in this paper by subclass, as PFSA or PFCA. A list of

environmentally relevant PFAAs compiled by Kurtz et al. (2019) are included in table 1.1. This experimental study, however, only tests PFOA, PFNA, PFDA and PFOS.

Table 1.1. Names, Number of Carbons, and Chemical Structures of Common PFAAs. (from Kurtz 2014)

PFC Name	Abbreviation	Number of Carbons	Structure
PFCAs			
Perfluorobutyric acid	PFBA	4	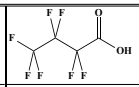
Perfluoropentanoic acid	PFPeA	5	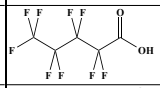
Perfluorohexanoic acid	PFHxA	6	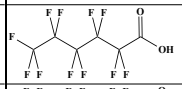
Perfluoroheptanoic acid	PFHpA	7	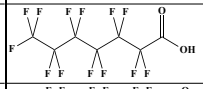
Perfluorooctanoic acid	PFOA	8	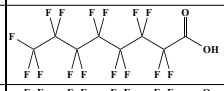
Perfluorononanoic acid	PFNA	9	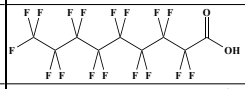
Perfluorodecanoic acid	PFDA	10	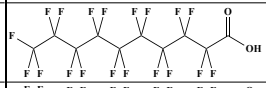
Perfluoroundecanoic acid	PFUnA	11	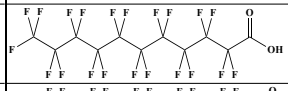
Perfluorododecanoic acid	PFDoA	12	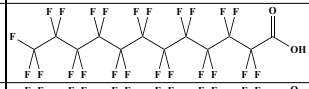
Perfluorotridecanoic acid	PFTriA	13	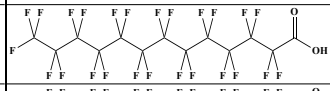
Perfluorotetradecanoic acid	PFTA	14	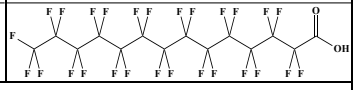
PFSAs			
Perfluorobutane sulfonate	PFBS	4	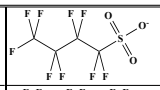
Perfluorohexane sulfonate	PFHxS	6	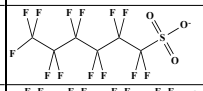
Perfluorooctane sulfonate	PFOS	8	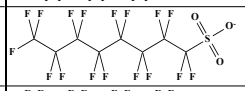
Perfluorooctane sulfonamide	PFOSA	8	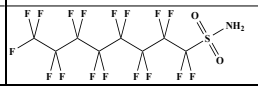

PFAA Sources

Emissions from manufacturing are the primary source of PFAAs (Armitage et al., 2009). These emissions are released into the atmosphere as gas or into water systems as wastewater (Armitage et al., 2009). PFAAs can also be indirectly introduced into the environment as precursor compounds that subsequently break down into the different PFAA compounds (Armitage et al., 2009). For example, the breakdown of a single precursor like ammonium perfluorooctanoate results in PFAAs of varying molecular composition and chain length (Armitage et al., 2009). The commercial manufacturing of ammonium perfluorooctanoate (APFO) and perfluoronaoanoate (APFN) as processing aids in the production of fluoropolymers yield the highest input of PFAAs into the environment (Armitage et al., 2009).

The manufacturing of PFAAs has changed in the United States since production started in the 1950s. From 2000 to 2002, the major PFAA manufacture, 3M Co., voluntarily phased out the manufacturing of PFOS (Rumsby et al., 2009). In 2006, the Environmental Protection Agency invited eight manufacturers to reduce the production of PFOA to 95% by 2010 and completely phase out the production of PFOA by 2015, as part of the Stewardship Program. These manufacturing companies included Arkema, Asahi, BASF Corporation, Clariant, Daikin, 3M Co., DuPont and Solvay Solexis. Additionally, PFOS and related substances were listed as Persistent Organic Pollutants in Annex B of the International Stockholm Convention in 2009.

PFAAs are distributed globally and have even been found in very remote locations (Houde et al., 2006). Even though PFOS is no longer produced in the United States, PFOS still remains the dominant PFAA found in species around the world (Houde et al., 2011). However, individual species have different concentration profiles, and the concentrations of individual compounds vary widely between species (Kannan et al., 2006). In general, PFAA concentrations

have been shown to be around 100 times higher in the northern hemisphere than the southern hemisphere (Houde et al., 2011). Houde et al. (2011) suggest that PFOA and PFOS levels are greater than 1200 ng/g ww in the liver in the Arctic, Europe, and Asia, because PFOA and PFOS precursors were still used in manufacturing in the northern hemisphere until they were phased out in 2015. While PFAAs are the most abundant, with recorded concentrations greater than 1200 ng/g ww in the liver near manufacturing areas in the northern hemisphere, they are also found in remote locations (Houde et al., 2011). Houde et al. (2011) conclude that these results support atmospheric deposition as a contamination source.

The long range atmospheric transfer of PFAAs has been debated; however, there has been an increase in evidence that PFAAs are transported globally through both the atmosphere and the ocean (Armitage et al, 2006). Modeling done by Armitage et al. (2009) shows that the transport of these compounds is dependent on carbon chain length. PFAAs with longer chain lengths transfer more efficiently through the air due to their air-water partition coefficient (K_{aw}) (Armitage et al., 2009). Their model shows that direct sources of contamination have higher impacts in the industrialized regions of the northern hemisphere. Dreyer et al. (2009) conclude that in remote locations long range transportation of these chemicals is an important mechanism for contamination. Conclusions of Dreyer et al.(2009) are supported by the model of Armitage et al. (2009), which showed that contamination movement in the arctic is highly dependent on molecular structure. This is consistent with the suggestion of Houde et al. (2011) that PFAAs reach remote locations by long-range atmospheric transport. Chain length determines whether these chemicals are reaching the arctic through the two modes of long-range transport: oceanic transport or atmospheric transport (Armitage et al., 2009). Longer chain PFAAs, because of their efficient transfer through air, are being transported to remote places through atmospheric

transport in higher concentrations than would be seen if they were being transported through the water alone.

Temporal Trends

Establishing general temporal trends in PFAA distribution is difficult because trends vary between locations and species. The proportion of PFSA concentration was shown to decrease in melon-headed whales by 24% from 1982-2006 (Houde et al., 2011). Conversely, PFOS concentrations in southern sea otter livers increased from 1992 to 1998 and then decreased after 2000. PFCA concentration was shown to increase by 24% in the same time period in melon-headed whales. Kurtz et al. (2019) found no clear temporal trend in samples collected from 1997 to 2013 from stranded cetaceans in the main Hawaiian Islands, Micronesia, Saipan, and Guam. In Alaska sea otters, the concentration of PFNA increased by a factor of 10 between 2004 and 2007 (Houde et al., 2011). These trends are reflected in American sea otters in California, but are very different from ones in Asia and Russia (Houde et al., 2011). The trends suggest concentrations are heavily source dependent; however, some general trends can be drawn. Houde et al. (2011) concludes that worldwide PFCA levels are increasing and may surpass PFSA levels if emission trends stay consistent.

Comparing temporal trends around the world is further complicated by the lack of an international standardized analytical method for sampling. To be able to reach a better understanding of how these levels are changing world wide an international standardized analytical method for sampling needs to be established, as suggested by Lau et al. (2011).

PFAAs are stored in protein rich tissues (Condor et al., 2007), and therefore the same temporal trends are not observed in the plasma and blubber as some of the other highly studied

toxicants in marine mammals. Toxicants sequestered in the blubber during the winter months are released into the bloodstream in the summer (Debeir et al., 2006). Since PFAAs are not stored in the blubber, this seasonal increase in PFAAs in plasma is not observed. Houde et al. (2006) found that plasma concentrations of PFAAs were higher during the summer of 2003, but that these values were not significantly different from the winter of 2004. Additionally, although blubber thickness varies temporarily, PFAA concentration in blubber has not been correlated to blubber thickness (Houde et al., 2006). Instead, Houde et al. (2006) showed that PFAA bioavailability in plasma was not increased by the metabolism of blubber (Houde et al., 2006). Therefore the distribution of PFAAs in marine mammal tissues directly affects the temporal trends observed.

Bioaccumulation and Biomagnification

PFAAs have been shown to bioaccumulate in bottlenose dolphins in the liver, kidneys, and blood (Condor et al., 2007). These patterns are different from ones seen in other persistent organic pollutants that collect in fatty tissues such as polychlorinated biphenyls, PCBs. Unlike lipophilic PCBs, PFAAs are proteinophilic and associate strongly with proteins (Condor et al., 2007). Therefore, they accumulate by orders of magnitude higher in areas that have a high concentration of proteins such as the liver, kidneys, and blood than other body compartments (Condor et al., 2007). Thus, PFAAs affect different parts of the body than PCBs, and it is important to understand these differences to determine the body burden of different toxicants.

Houde et al. (2011) assert traditional bioaccumulation models are inappropriate for quantifying accumulation factors, because PFAAs associate with proteins and not lipids. Traditional methods use the equilibrium partition coefficient of octanol-water (log K_{ow}), which

describes the chemicals tendency to migrate from water to lipid (Houde et al., 2011). Other bioaccumulation models such as OMEGA have shown that the uptake of PFOS is comparable to moderately hydrophobic compounds (Houde et al., 2011). The elimination of PFOS was comparable to that of short to medium chain fatty acids (Houde et al., 2011).

The correct quantification of accumulation factors is important for the regulation of PFAA manufacturing (Conder et al., 2007). Current regulations use the equilibrium partitioning coefficient of octanol-water (log K_{ow}) of contaminants to classify and regulate materials (Conder et al., 2007). Since the potential for these contaminants to bioaccumulate is misrepresented using the current models, the regulation of these compounds is also affected (Conder et al., 2007). This suggests that the current basis for management and regulation is inaccurate and may not be doing enough to reduce animal body burdens.

Kelly et al. (2009) describes four reasons why these compounds show such a high degree of bioaccumulation. Efficient dietary assimilation in marine mammals and other mammals prevents initial excretion of these compounds (Kelly et al., 2009). PFAAs are retained in protein rich tissues and fluids instead of being efficiently eliminated (Kelly et al., 2009). PFAAs have a high resistance to metabolism, which prevents the breakdown and excretion of smaller molecules (Kelly et al., 2009). Finally, PFAAs have a low volatility, which relates to high gastrointestinal uptake and low elimination (Kelly et al., 2009). The combination of these factors leads to the high concentrations of PFAAs seen in bottlenose dolphins.

PFAAs also biomagnify in food webs, meaning contaminant concentrations increase with trophic level. Even lower trophic-level organisms were found to have concentrations of PFOS three magnitudes greater than surface waters in the great lakes (Kannan et al., 2004). This amplification, seen at lower levels, continues to increase up the food chain. The magnification

can be described by trophic magnification factors (TMFs) which indicate biomagnification when greater than one (Kelly et al., 2009). In Arctic marine mammal food web, TMFs were between 5 and 14 (Kelly et al., 2009). Similar results have been demonstrated in vastly different food webs. The Great Lakes, Charleston, South Carolina, Sarasota Bay, the Eastern Arctic and Lake Ontario have vastly different temperatures and food web structures, yet similar TMF values have been found in each area (Houde et al., 2011). Thus each geographic region shows biomagnification, even though individual locations differ greatly in trophic structure.

The bioaccumulation of individual PFAAs can differ depending on the compound length and functional group (Conder et al., 2007). Conder et al. (2007) describe the following five factors that affect bioaccumulation of PFCAs specifically. First, longer chain lengths are more likely to bioaccumulate. Second, they note that PFSAs bioaccumulate more than PFCAs of the same carbon length. According to regulator criteria of 1000-5000 L/kg, PFCAs with seven fluorinated carbons or less do not bioaccumulate (Conder et al., 2007). Thus, PFCAs with seven fluorinated carbons or less have very low biomagnification potential in food webs. Finally, they conclude that more research needs to be done on PFCAs with a carbon chain greater than seven to characterize bioaccumulation factors. These results are why PFCAs with chain lengths of seven are more commonly observed than those with fewer. However, there is a potential that PFCAs with fewer carbons still add to the overall body burden that is possibly being overlooked.

The biomagnification factors of PFCAs with carbon chains greater than seven have been demonstrated in multiple studies; however, the degree of biomagnification is highly influenced by how the trophic magnification factor is calculated. PFAA concentrations are usually measured using the liver and plasma values as a wet weight. Houde et al. (2006) suggest that these values overestimate the bioaccumulation factor when they are used with whole body homogenates from

other species. Instead they recommend extrapolating to the total body concentration using the total body weight, organ weights and blood plasma volume to accurately measure TMF. When comparing concentration values using levels reported from the liver and from total body, they found concentrations in the liver to be nine times higher than calculated values for whole body concentrations in belugas and narwhals. Therefore, Kannan et al. (2006) and Kelley et al. (2009) and other studies that use liver concentrations instead of total body concentrations overestimate TMF values. This overestimate has implications for regulations and management.

Life History Traits

As a whole, juvenile dolphins have higher PFAA concentrations in plasma than adults. Concentrations of PFCAs with eight to twelve carbons, PFOS, and PFHxS were shown to be significantly higher in juvenile dolphins than adults, and the concentration of these compounds was negatively correlated with age (Houde et al., 2006). These authors also suggested that the lower concentrations observed in adults are a result of increased elimination capabilities, changes in diet, and changes in habitat. Similar results have been seen in immature seals. Short-chain PFAAs were present in seal pups that were not present in adults (Houde et al., 2011). However, in a different study where age ranges were separated into three classes, calves, juveniles and adults, juveniles had higher concentrations than both adults and calves (Kurtz et al., 2019). These results suggest differences in juvenile ability to metabolize and eliminate these toxicants (Houde et al., 2011).

Adult females and males have similar concentrations of PFAAs. This trend is very different from other contaminants such as polychlorinated biphenyls, which have been shown to significantly decrease in only adult females (Houde et al., 2006). In the same study both adult

females and adult males were observed to have decreased concentrations of PFAAs in plasma with increasing age. The authors concluded that differences in habitat, diet and or more efficient elimination could explain the differences in PFAAs seen with age. Another potential explanation of decreased concentration levels in adult females is the transfer of PFAAs from pregnant mothers through gestation and lactation. Houde et al. (2006) suggests that PFAA transfer from the mother occurs with the first calf. This idea is supported by concentrations measured in females in this study. Concentrations were lower in females that were seen with one calf than those not been documented with a calf. Additionally, mothers of multiple calves do not have significantly lower concentrations than those with only one calf.

The elimination of PFAAs through lactation has also been supported by the analysis of milk samples (Houde et al., 2006). PFOA, PFNA, PFDA, PFUA, PFDoA, PFOSA, PFHxS, PFTA, and PFOS were all found in milk samples at varying concentrations. PFOS was the predominant compound found, with concentrations up to 100 times greater than the other contaminants. Since PFOS have been shown to bind strongly to proteins, milk serves as a good pathway for PFAA transfer. There is a potential for placental transfer of PFAAs as well, which was observed in rodents and harbor porpoise (Houde et al., 2006).

While Houde et al. (2006) describe multiple routes for PFAA transfer from mother to calf, they do not account for the similar concentration decrease in adult males and adult females that have given birth. Adult females with one calf were seen to have lower concentrations, yet the similarity between adult males and adult females suggests that PFAA offloading by females does not significantly reduce female toxicant load in the same way that transfer of PCBs does (Houde et al., 2006). This inconsistency suggests another factor is involved in female PFAA concentration during pregnancy. Possible explanations could be reduced ability to eliminate

PFAAs through urine and feces during pregnancy or increased uptake of PFAAs during pregnancy. Another explanation is that PFAA elimination through transfer to offspring does not reduce PFAA concentration in females enough to be statistically significant when compared to males.

Habitat and local exposure also have been demonstrated to affect the concentration of PFAAs in different dolphin populations. Higher concentrations were found in dolphins from Charleston, South Carolina than those in Indian River Lagoon, Florida (Fair et al., 2012). These concentrations suggest that point sources of pollution from more urbanized areas such as Charleston, South Carolina may compound the exposure of these compounds (Fair et al., 2012). This result is consistent with Armitage et al.'s (2009) model that shows effects of contamination to be higher in industrialized areas.

PFAA Elimination

Elimination of PFAAs has been documented in dolphin urine. For compounds with carbon chain lengths between 8 and 11 carbons, Houde et al. (2006) found that compounds with fewer numbers of carbons were excreted more easily through urine. This finding was consistent with smaller concentrations of compounds that are less easily excreted found in plasma samples. While large amounts of PFAAs may be excreted through urine, Houde et al. (2006) observed that the intake of PFOS still exceeds the estimated excretion concentration.

Although dolphins excrete PFOS, the rates of environmental input may be too high for animals to eliminate these toxicants at the same rate they are ingesting them. Houde et al. (2006) implied that there may be a concentration threshold beyond which dolphins cannot eliminate a toxicant, they do not speculate whether processing even small amounts of these compounds has a

negative effect on dolphin health. It remains unclear whether concentrations below this excretion threshold still produce negative health effects, or if health effects occur only after a threshold level of PFAA accumulation.

No sex or age-related differences were seen in the elimination of PFAAs through dolphin urine (Houde et al., 2006); however, testosterone was shown to limit PFOA elimination in rat urine (Kudo et al., 2001). Female and castrated male rats have similar elimination concentrations, while males eliminate less PFOA through urine (Kudo et al., 2001). Additionally, females treated with testosterone showed depression of PFOA elimination (Kudo et al., 2001). Houde et al. (2006) found very low concentrations of PFOA in urine, and in more than 84% of the samples it was below the method detection limit. They conclude that the low detection rate may have affected the results and resulted in no relationship between concentration and sex. Therefore, additional studies need to be conducted to determine if there is a relationship between sex and elimination of PFAAs in urine at lower concentrations.

In rats, 5% of injected PFCAs were eliminated in feces within 120 hours (Kudo et al., 2001). In the same study, 92% of the injected PFCAs were eliminated in urine. Additionally, Kudo et al. found that there was no difference between female and male excretion of PFCAs in feces. The relationship seen in other mammals suggests that feces could be a possible PFAA excretion method for dolphins, although it may be a less effective pathway compared to urine.

Toxicological Effects

Most of the information about the toxicological impact of PFAAs comes from the two compounds PFOA and PFOS, because of the high proportion of these chemicals in the environment (Corsini et al., 2014). PFOA can be classified as an endocrine disruptor, a chemical

that affects hormones by modifying the synthesis, circulating levels and peripheral action (Lunardi et al., 2016). Kannan et al. (2006) describes PFOA and PFOS as peroxisome proliferators, because they have been shown to suppress immune response in mice. In lab-tested animals, these two compounds were shown to cause a wide range of serious effects including: liver, testicular, and pancreatic tumors, reproductive and developmental deficits, neurotoxicity and immunotoxicity (Corsini et al., 2014).

Lundardi et al. (2016) subjected dolphin skin biopsies to PFOA and confirmed possible pathways in gene regulation responsible for the adverse toxicological effects. Of the 428 genes that were differentially regulated with exposure to PFOA in this study, 191 were upregulated and 237 were downregulated. Lundardi et al., classified these genes into the following categories: cellular processes (32.5%), metabolic process (27.4%), single organism process (25.7%), biological regulation (20.5%), immune system process (2.6%), cellular component organization or biogenesis (15.4%), localization (12.8%), multicellular organismal process (9.4%), and developmental process (8.5%).

Lundardi et al. (2006) compared the up and down regulation of specific genes to known toxicological effects of PFOA. For instance, humans exposed to high levels of PFOA show changes in clinical markers of immune and inflammatory processes. These health effects support their findings that *complement c*5, which mediates local inflammatory processes, was downregulated. Similarly, they compared the upregulation of *vascular endothelial growth factor* and *Rho GTPase-activating protein* with effects of PFOA exposure. These two genes are involved with the development of the central nervous system. The upregulation of these genes is consistent with the findings that exposure to PFOA during pregnancy causes reduced body weight and neonatal mortality in mice (Lundardi et al., 2006).

Kannon et al. (2006) demonstrate a link between PFAA concentrations and disease in sea otters. PFOA and PFOS concentrations were significantly higher, $p < 0.05$, in stranded sea otters that had infectious diseases. They conclude that the association between disease and PFAA concentration does not imply causality. Although there is a significant association, it is still unknown if higher concentration levels increase the susceptibility to disease, or if the higher concentration levels are a result of the disease. Additionally, it is possible a third factor increases both the susceptibility of disease and increased concentration level.

The same study by Kannan et al. (2006) show that hepatic concentrations of PFAAs are not correlated to emaciated body conditions. Concentrations of PFOS and PFOA in the sea otters studied were not significantly different, $p < 0.05$, between noninfectious and emaciated otters. This finding differs from PCB contaminants, which are mobilized from lipid storage during starvation. It is also consistent with the findings of other studies, such as Condor et al. (2007), that conclude that PFAAs are stored in protein rich tissues and not lipids. Kannan et al. (2006) conclude that fat mobilization has little to no effect on PFAA distribution in sea otter tissues.

Potential Protein Biomarkers PPARα and CYP4A

PPARα

The protein PPARα is a peroxisome proliferator-activated receptor in a class of ligand-activated transcription factors of the steroid/thyroid nuclear superfamily. Three subtypes of PPAR proteins, PPARα, PPARβ, and PPARγ have been identified in rodents and humans (Devchand et al., 1996). PPARs regulate many cellular processes including energy metabolism, cell differentiation, and the expression of genes associated with lipid homeostasis (Wolf et al., 2008; Devchand et al., 1996). PPARα's primary roles include lipid homeostasis, fatty acid

catabolism, peroxisome proliferation and inflammation (Wolf et al., 2008). In addition, PPARα has the ability to mediate a pleiotropic response to peroxisome proliferators (Devchand et al., 1996).

PPARα is primarily expressed in the liver, but expression is also seen in the kidney, brown adipose tissue, eye, digestive tract, immune and genital systems (Devchand et al., 1996). Tissues that express these proteins have high fatty acid catabolism (Devchand et al., 1996).

In vitro, PFAAs have been shown to activate PPARα in both mice and human cell lines (Wolf et al., 2008, Heuvel et al., 2006). Activation of PPARα induced peroxisomal enzymes in male rats, inhibited peroxisomal beta-oxidation in female rats, and induced peroxisome proliferation in both rats and mice (Wolf et al., 2008). This is consistent with PPARα- mediated responses as PFOA is an immunosuppressive in mice and anti-inflammatory in rats (Wolf et al., 2008).

The magnitude of response to PFAA induced PPARα induction is dependent on the chain length of the carbon backbone and the functional group of the PFAA (Wolf et al., 2008). Wolf et al. (2008) found that in general increasing chain length of the carboxylate, up to C9, increased the activation of PPARα. This is consistent with other studies that report increased hepatomegaly and peroxisomal beta-oxidation with increasing chain length of PFAA exposure (Wolf et al., 2008). Carboxylates also induce higher activity of PPARα than sulfonates (Wolf et al., 2008). Since PFAAs of fewer than eight carbons can be eliminated through urine (Houde et al., 2006) and PFAAs with longer chain lengths are more bioaccumulative (Conder et al., 2007), this suggests that PFAAs with longer chain lengths have more potential to have toxic effects.

While an increased expression of PPARα with exposure to perfluoroalkyl acids has been documented in mice, humans and Baikal seals (Wolf et al., 2008; Ishibashi et al., 2008), the

mechanism of activation is unknown. Other compounds that activate this pathway include fibrates, fatty acids and eicosanoids (Devchand et al., 1996).

While it has been documented that PFAAs induce PPARα activation in multiple mammal species, the sensitivity to these compounds has varied across species. The activation of mouse PPARα is higher for all PFAAs than the activation of PPARα in human cells (Wolf et al., 2008). This suggests that there are differences in the PPARα pathway between mammal species. PPARα mRNA expression positively correlated with concentration of PFTriA, PFTA, PFDA, and PFUnA in the kidney of stranded Hawaiian cetaceans, suggesting that the PPARα-CYP4A pathway is not only conserved in cetaceans, but PPARα protein expression may also be affected by PFAAs (Kurtz et al., 2019).

CYP4A

The CYP4 family has eleven subfamilies, which encode isozymes that are expressed in mammals (Simpson, 1997). Cytochrome P450 enzymes catalyze the hydroxylation of the terminal ω-carbon and to the lesser extent the ω-1 position of saturated and unsaturated fatty acids (Simpson, 1997). The omega (ω)-hydroxylation creates a polar alcohol metabolite by transforming the terminal methyl group of a hydrophobic aliphatic chain (Johnson et al., 2015). This catalytic step initiates formation of monocarboxylic acids and dicarboxylic acids that are subsequently catabolized in the beta-oxidation pathway (Johnson et al., 2015). This pathway may prevent the toxic buildup of fatty acids in the body, and is essential for the anabolism and catabolism of critical lipid mediators, such as leukotriene (Johnson et al., 2015). Additionally, the ω-hydroxylation pathway has been linked with many disease processes such as inflammation and cancer progression (Johnson et al., 2015).

Peroxisome proliferators, including PPARα, induce the expression of CYP4A. Disruption of the PPARα-CYP4A pathway by PFAAs has been demonstrated in different mammal species. In rodents, the expression of CYP4A was induced by PFOS (Hu et al., 2005), although the pathway for activation induced by perfluoroalkyl acids is still unknown. Additionally, the expression of hepatic CYP4A-like protein was significantly correlated with concentrations of PFNA and PFDA in wild Baikal seals (Ishibashi et al., 2008). Through their work with cells transfected with wild Baikal Seal cDNA, Ishibashi et al. (2008) concluded that the PPARα-CYP4A pathway could be a potential biomarker for evaluating PFAA biological effects in wildlife. Kurtz et al. (2019) also found a significant correlation between CYP4A protein expression and PFAA concentration in stranded Hawaiian cetaceans.

PFAA exposure modulates the PPARα-CYP4A signaling pathway by increasing the expression of PPARα and CYP4A in other mammals (Cheng and Klaassen, 2008; Wolf et al., 2008; Hu et al., 2005; Rosen et al., 2008). Two studies have examined the relationship between PFAA exposure and the PPARα-CYP4A signaling pathway in marine mammals. Kurtz et al., (2019) found a significant correlation between high PFAA concentrations in stranded cetacean tissues and PPARα and CYP4A expression. Additionally, Ishibashi et al. (2008) demonstrated that the PPARα-CYP4A signaling pathway has the potential for use as an effective biomarker for PFAA exposure in wild Baikal seals. However, since both of these studies used wild animals there is the potential for other factors to be influencing the expression of the PPARα-CYP4A signaling pathway.

Understanding how PFAA exposure impacts cetacean health can lead to better management practices and environmental protection for cetaceans and other organisms exposed

to PFAAs. Developing reliable biomarkers to indicate exposure to PFAAs in cetaceans is an important step in understanding how these chemical contaminants affect marine mammal health.

References:

Abbott, B. (2009). Review of the expression of peroxisome proliferator-activated receptors alpha (PPARα), beta (PPARβ), and gamma (PPARγ) in rodent and human development. *Reproductive Toxicology*, 27, 246-257.

Abbott B. D., Wolf C. J., Das K. P., Zehr R. D., Schmid J. E., Lindstrom A. B., Strynar M. J., & Lau C. (2009). Developmental toxicity of perfluorooctane sulfonate (PFOS) is not dependent on expression of peroxisome proliferator activated receptor-alpha (PPAR alpha) in the mouse. Reproductive Toxicology, 27(3-4), 258-265.

Abbott, B. A., Wolf, C. J., Schmid, J. E., Das, K. P., Zehr, R. D., Helfant, L., Nakayama, S., Lindstrom, A. B., Strynar, M. J., and Lau, C. (2007). Perfluorooctanoic acid-induced developmental toxicity in the mouse is dependent on expression of perioxisome proliferator-activated receptor-alpha. Toxicological Sciences, 98(2), 571-581.

Adams, J., Houde, M., Muir, D., Speakman, T., Bossart, G., & Fair, P. (2008). Land use and the spatial distribution of perfluoroalkyl compounds as measured in the plasma of bottlenose dolphins (Tursiops truncatus). Marine Environmental Research, 66(4), 430-437.

Ahrens, L., Marusczak, N., Rubarth, J., Dommergue, A., Nedjai, R., Ferrari, C. & Ebinghaus, R. (2010). Distribution of perfluoroalkyl compounds and mercury in fish liver from high-mountain lakes in France originating from atmospheric deposition. Environmental Chemistry, 7, 422–428.

Ahrens, L., Siebert, U., & Ebinghaus, R. (2009). Total body burden and tissue distribution of polyfluorinated compounds in harbor seals (Phoca vitulina) from the German Bight. Marine Pollution Bulletin, 58(4), 520-525.

Aldridge, T. C., Tugwood, J. D., & Green, S. (1995). Identification and characterization of DNA elements implicated in the regulation of CYP4A1 transcription. Biochemical Journal, 306(Pt 2), 473.

Anderson, A. (2008). The induction of CYP2B proteins in rodents by phenobarbital-like inducers: what has been discovered and what remains to be learned. Acta Chimica Slovenica, 55(1), 45.

Apelberg, B., Goldman, L., Calafat, A., Herbstman, J., Kuklenyik, Z., Heidler, J., Needham, L., Halden, R., & Witter, F. (2007). Determinants of fetal exposure to polyfluoroalkyl compounds in Baltimore, Maryland. Environmental Science & Technology, 41(11), 3891-3897.

Armitage, J. M., MacLeod, M., & Cousins, I. T. (2009). Comparative assessment of the global fate and transport pathways of long-chain perfluorocarboxylic acids (PFCAs) and

perfluorocarboxylates (PFCs) emitted from direct sources. Environmental Science & Technology, 43(15), 5830-5836.

Asakawa, A., Toyoshima, M., Harada, K., Fujimiya, M., Inoue, K., and Koizumi, A. (2008). The ubiquitous environmental pollutant perfluoroctanoic acid inhibits feeding behavior via peroxisome proliferator-activated receptor-alpha. International Journal of Molecular Medicine, Apr. 21 (4), 439-45.

Berger, J. & Moller, D. (2002). The Mechanisms of Actions of PPARs. Annual Review of Medicine, 53, 409-435.

Betts, K. S. (2007). Perfluoroalkyl acids: what is the evidence telling us?. Environmental Health Perspectives, 115(5), A250.

Cheng, X. and Klaasen, C. D. (2008). Perfluorocarboxylic Acids Induce Cytochrome P450 Enzymes in Mouse Liver through Activation of PPAR-α and CAR Transcription Factors. Toxicological Sciences, 106(1), 29.

Conder, J. M., Hoke, R. A., Wolf, W. d., Russell, M. H., & Buck, R. C. (2008). Are PFCAs bioaccumulative? A critical review and comparison with regulatory criteria and persistent lipophilic compounds. Environmental Science & Technology, 42(4), 995-1003.

Corsini, E., Luebke, R. W., Germolec, D. R., & DeWitt, J. C. (2014). Perfluorinated compounds: Emerging POPs with potential immunotoxicity. Toxicology Letters, 230(2), 263-270.

Devchand, P. R., Keller, H., Peters, J. M., Vazquez, M., Gonzalez, F. J., & Wahli, W. (1996). The PPAR [alpha]-leukotriene B4 pathway to inflammation control. Nature, 384(6604), 39.

Debier, C., Chalon C Fau - Le Boeuf, B. J., Le Boeuf Bj Fau - de Tillesse, T., de Tillesse T Fau - Larondelle, Y., Larondelle Y Fau - Thome, J.-P., & Thome, J. P. (2006). Mobilization of PCBs from blubber to blood in northern elephant seals (Mirounga angustirostris) during the post-weaning fast. Aqua Toxocol, 16;80(2):149-57.

Dreyer, A., Weinberg, I., Temme, C., & Ebinghaus, R. (2009). Polyfluorinated compounds in the atmosphere of the Atlantic and Southern Oceans: evidence for a global distribution. Environmental Science & Technology, 43(17), 6507-6514.

Fair, P. A., Houde, M., Hulsey, T. C., Bossart, G. D., Adams, J., Balthis, L., et al. (2012). Assessment of perfluorinated compounds (PFCs) in plasma of bottlenose dolphins from two southeast US estuarine areas: relationship with age, sex and geographic locations. Marine Pollution Bulletin, 64(1), 66-74.

Fossi, M. C., Casini, S., Bucalossi, D., & Marsili, L. (2008). First detection of CYP1A1 and CYP2B induction in Mediterranean cetacean skin biopsies and cultured fibroblasts by Western blot analysis. Marine Environmental Research, 66(1), 3-6.

Houde, M., Balmer, B. C., Brandsma, S., Wells, R. S., Rowles, T. K., Solomon, K. R., et al. (2006). Perfluoroalkyl compounds in relation to life-history and reproductive parameters in bottlenose dolphins (Tursiops truncatus) from Sarasota Bay, Florida, USA. Environmental Toxicology and Chemistry, 25(9), 2405-2412.

Houde, M., De Silva, A. O., Muir, D. C., & Letcher, R. J. (2011). Monitoring of perfluorinated compounds in aquatic biota: An updated review: PFCs in aquatic biota. Environmental Science & Technology, 45(19), 7962-7973.

Hu, W., Jones, P. D., Celius, T., & Giesy, J. P. (2005). Identification of genes responsive to PFOS using gene expression profiling. Environmental Toxicology and Pharmacology, 19(1), 57-70.

Intrasuksri, U., Rangwala, S. M., O'Brien, M., Noonan, D. J., & Feller, D. R. (1998). Mechanisms of peroxisome proliferation by perfluorooctanoic acid and endogenous fatty acids. General Pharmacology, 31, 187–197.

Ishibashi, H., Iwata, H., Kim, E., Tao, L., Kannan, K., Tanabe, S., Batoev, V. B., & Petrov, E. A. (2008). Contamination and Effects of Perfluorochemicals in Baikal Seal (Pusa sibirica). 2. Molecular Characterization, Expression Level, and Transcriptional Activation of Peroxisome Proliferator-Activated Receptor α. Environmental Science & Technology, 42(7), 2302-2308.

Ishibashi, H., Kim, E., & Iwata H. (2011). Transactivation Potencies of the Baikal Seal (Pusa sibirica) Peroxisome Proliferator-Activated Receptor α by Perfluoroalkyl Carboxylates and Sulfonates: Estimation of PFOA Induction Equivalency Factors. Environmental Science & Technology, 45(7), 3123-3130.

Johnson, A. F., Johnson, A. L., Edson, K. F., Edson, K. Z., Totah, R. F., Totah, R. A., & Rettie A. F., Rettie, A. E., Cytochrome P450 ω-Hydroxylases in Inflammation and Cancer. (1054-3589 (Print)).

Jones, P. D., Hu, W., De Coen, W., Newsted, J. L., & Giesy, J. P. (2003). Binding of perfluorinated fatty acids to serum proteins. Environmental Toxicology and Chemistry, 22(11), 2639-2649.

Kannan, K., Koistinen, J., Beckmen, K., Evans, T., Gorzelany, J. F., Hansen, K. J., Jones, P. D., Helle, E., Nyman, M. & Giesy, J. P. (2001). Accumulation of perfluorooctane sulfonate in marine mammals. Environmental Science & Technology, 35(8), 1593-1598.

Kannan, K., Perrotta, E., & Thomas, N. J. (2006). Association between perfluorinated compounds and pathological conditions in southern sea otters. Environmental Science & Technology, 40(16), 4943-4948.

Kannan, K., Tao, L., Sinclair, E., Pastva, S. D., Jude, D. J., & Giesy, J. P. (2005). Perfluorinated compounds in aquatic organisms at various trophic levels in a Great Lakes food chain. Archives of Environmental Contamination and Toxicology, 48(4), 559-566.

Kelly, B. C., Ikonomou, M. G., Blair, J. D., Surridge, B., Hoover, D., Grace, R., et al. (2009). Perfluoroalkyl contaminants in an Arctic marine food web: trophic magnification and wildlife exposure. Environmental Science & Technology, 43(11), 4037-4043.

Kudo, N., Suzuki, E., Katakura, M., Ohmori, K., Noshiro, R., & Kawashima, Y. (2001). Comparison of the elimination between perfluorinated fatty acids with different carbon chain length in rats. Chemico-biological Interactions, 134(2), 203-216.

Kurtz, A. E., Reiner, J. L., West, K. L., & Jensen, B. A. (2019). Perfluorinated Alkyl Acids in Hawaiian Cetaceans and Potential Biomarkers of Effect: Peroxisome Proliferator-Activated Receptor Alpha and Cytochrome P450 4A. Environmental Science & Technology, 53(5), 2830-2839.

Lau, C., Anitole, K., Hodes, C., Lai, D., Pfahles-Hutchens, A., & Seed, J. (2007). Perfluoroalkyl Acids: A Review of Monitoring and Toxicological Findings. Toxicological Sciences, 99(2), 366-394.

Lemal, D., M. (2004). Perspective on fluorocarbon chemistry. Journal of Organic Chemistry, 69(1), 1-11.

Lunardi, D., Abelli, L., Panti, C., Marsili, L., Fossi, M. C., & Mancia, A. (2016). Transcriptomic analysis of bottlenose dolphin (Tursiops truncatus) skin biopsies to assess the effects of emerging contaminants. Marine Environmental Research, 114, 74-79.

Maloney, E. & Waxman, D. (1999). trans-Activation of PPARα and PPARγ by structurally diverse environmental chemicals. Toxicology and Applied Pharmocology, 161, 209-218.

Mangelsdorf, D. J. & Evans, R. M. (1995). The RXR heterodimers and orphan receptors. Cell, 83, 841–50.

Moore, L. B., Maglich, J. M., McKee, D. D., Wisely, B., Willson, T. M., Kliewer, S. A., et al. (2002). Pregnane X receptor (PXR), constitutive androstane receptor (CAR), and benzoate X receptor (BXR) define three pharmacologically distinct classes of nuclear receptors. Molecular Endocrinology, 16(5), 977-986.

Niimi, S., Kim, E. Y., Iwata, H., Watanabe, M. X., Yasunaga, G., Fujise, Y., & Tanabe, S. (2007). Identification and hepatic expression profiles of cytochrome P450 1–4 isozymes in common minke whales (Balaenoptera acutorostrata). Comparative Biochemistry and Physiology Part B: Biochemistry and Molecular Biology, 147(4), 667-681.

Pistocchi, A., & Loos, R. (2009). A map of European emissions and concentrations of PFOS and PFOA. Environmental Science & Technology, 43(24), 9237-9244.

Prevedouros, K., Cousins, I. T., Buck, R. C., & Korzeniowski, S. H. (2006). Sources, fate and transport of perfluorocarboxylates. Environmental Science & Technology, 40(1), 32-44.

Qazi, M.R., Xia, Z., Bogdanska, J., Chang, S.C., Ehresman, D.J., Butenhoff, J.L., Nelson, B.D., DePierre J.W., Abedi-Valugerdi, M., 2009. The atrophy and changes in the cellular compositions of the thymus and spleen observed in mice subjected to short-term exposure to perfluorooctanesulfonate are high-dose phenomena mediated in part by peroxisome proliferator-activated receptor-alpha (PPARalpha). Toxicology, 584 260, 68–76.

Rakhshandehroo, M., Knoch, B., Müller, M., & Kersten, S. (2010). Peroxisome Proliferator-Activated Receptor Alpha Target Genes. PPAR Research, 2010, 20.

Rayne, S. & Forest, K. (2009). Perfluoroalkyl sulfonic and carboxylic acids: A critical review of physicochemical properties, levels and patterns in waters and wastewaters, and treatment methods. Journal of Environmental Science and Health, A44(12), 1145-1199.

Renner, R. (2001). Growing concern over perfluorinated chemicals. Environmental Science & Technology, 35(7), 154A-160A.

Renner, R. (2006). The long and the short of perfluorinated replacements. Environmental Science & Technology, 40(1), 12-13.

Robertson, G., Leclercq, I., & Farrell, G. C. (2001). II. Cytochrome P-450 enzymes and oxidative stress. American Journal of Physiology-Gastrointestinal and Liver Physiology, 281(5), G1135-G1139.

Rosen, M. B., Lee, J. S., Ren, H., Vallanat, B., Liu, J., Waalkes, M. P., . . . Corton, J. C. (2008b). Toxicogenomic dissection of the perfluorooctanoic acid transcript profile in mouse liver: Evidence for the involvement of nuclear receptors PPARα and CAR. Toxicological Sciences, 103(1), 46-56.

Rumsby, P. C., McLaughlin, C. L., & Hall, T. (2009). Perfluorooctane sulphonate and perfluorooctanoic acid in drinking and environmental waters. Philosophical Transactions of the Royal Society A: Mathematical, Physical and Engineering Sciences, 367(1904), 4119-4136.

Shaw, S., Berger, M. L., Brenner, D., Tao, L., Wu, Q., & Kannan, K. (2009). Specific accumulation of perfluorochemicals in harbor seals (Phoca vitulina concolor) from the northwest Atlantic. Chemosphere, 74(8), 1037-1043.

Shipley, J., Hurst, C., Tanaka, S., DeRoos, F., Butenhoff, J., Seacat, A., & Waxman, D. (2004). Trans activation of PPARα and induction of PPARα target genes by perfluorooctane-based chemicals. Toxicological Sciences, 80, 151-160.

Simpson, A. E. C. M. (1997). The cytochrome P450 4 (CYP4) family. General Pharmacology: The Vascular System, 28(3), 351-359.

Singh, I. (1997). Biochemistry of peroxisomes in health and disease. Molecular and Cellular Biochemistry, 167(1-2), 1-29.

Tao, L., Kannan, K., Kajiwara, N., Costa, M. M., Fillmann, G., Takahashi, S., & Tanabe, S. (2006). Perfluorooctanesulfonate and related fluorochemicals in albatrosses, elephant seals, penguins, and polar skuas from the Southern Ocean. Environmental Science & Technology, 40(24), 7642-7648.

Timsit, Y. E., & Negishi, M. (2007). CAR and PXR: The xenobiotic-sensing receptors. Steroids, 72(3), 231-246.

Trumble, S. J., & Kanatous, S. B. (2012). Fatty Acid use in Diving Mammals: More than Merely Fuel. Frontiers in Physiology, 3, 184.

Vanden Heuvel, J. P., Thompson, J. T., Frame, S. R., & Gillies, P. J. (2006). Differential activation of nuclear receptors by perfluorinated fatty acid analogs and natural fatty acids: A comparison of human, mouse, and rat peroxisome proliferator-activated receptor-α,-β, and-γ, liver X receptor-β, and retinoid X receptor-α. Toxicological Sciences, 92(2), 476-489.

Van de Vijver, K. I., Hoff, P. T., Das, K., Van Dongen, W., Esmans, E. L., Jauniaux, T., Bouquegneau, J. M., Blust, R. & De Coen, W. (2003). Perfluorinated chemicals infiltrate ocean waters: link between exposure levels and stable isotope ratios in marine mammals. Environmental Science & Technology, 37(24), 5545-5550.

Wahli W., Braissant O., Desvergne B. (1995). Peroxisome proliferator activated receptors: transcriptional regulators of adipogenesis, lipid metabolism and more. Chemistry & Biology, 2, 261–66.

Waxman, D. J. (1999). P450 gene induction by structurally diverse xenochemicals: Central role of nuclear receptors CAR, PXR, and PPAR. Biochemistry and Biophysics, 369(1), 11-23.

Wolf, C. J., Takacs, M. L., Schmid, J. E., Lau, C., & Abbott, B. D. (2008). Activation of mouse and human peroxisome proliferator− activated receptor alpha by perfluoroalkyl acids of different functional groups and chain lengths. Toxicological Sciences, 106(1), 162-171.

Yang, Q., Xie, Y., Alexson, S., Nelson, B., & De Pierre, J. (2002). Involvement of the peroxisome proliferator-activated receptor alpha in the immunomodulation caused by peroxisome proliferators in mice. Biochemical Pharmacology, 63, 1893-1900.

Young, C. J., Furdui, V. I., Franklin, J., Koerner, R. M., Muir, D. C. G. & Mabury, S. A. (2007). Perfluorinated acids in Arctic snow: New evidence for atmospheric formation. Environmental Science & Technology, 41, 3455−3461.

Zushi, Y., Ye, F., Motegi, M., Nojiri, K., Hosono, S., Suzuki, T., Kosugi, Y., Yaguchi, K. & Masunaga, S. (2011). Spatially detailed survey on pollution by multiple perfluorinated compounds in the Tokyo Bay basin of Japan. Environmental Science & Technology, 45, 2887−2893.

CHAPTER 2:

An In Vitro Analysis of PPARα and CYP4A as Potential Biomarkers for Perfluoroalkyl Acid Exposure in Cetacean Kidney Cells.

Abstract

Concern for the high concentration of PFAAs seen in marine mammals has led to the investigation of the effect of these chemicals on their health. Two proteins have been suggested as potential biomarkers for PFAA exposure, peroxisome proliferator-activated receptor alpha (PPARα) and cytochrome P450 4A (CYP4A). PPARα is a transcription factor, which induces transcription of CYP4A, and PFAAs have been documented to activate PPARα in other mammals including mice, humans, and Baikal seals. Additionally, there is a correlation in cetaceans stranded in Hawaii between high concentrations of PFAAs and PPARα mRNA and CYP4A protein expression. We measured protein expression of PPARα and CYP4A in *Tursiops truncatus* kidney cells exposed *in vitro* to four PFAAs, PFOA, PFDA, PFOS, and PFNA. The relative expression of each protein was quantified using western blot. At the highest dose (225 uM), all four chemicals induced greater expression of PPARα than the vehicle control, but this increase in expression was not statistically significant ($p < 0.05$). There was a statistically significant difference between the protein expression of PPARα in cells exposed to the two lower concentrations of PFNA (1 uM and 25 uM) and the highest concentration (225 uM) ($p = 0.0288$). All four chemicals elicited a dose dependent response in expression of CYP4A; however, the change in expression was not significantly different between treatment groups and from the vehicle control ($p < 0.05$) with the exception of PFOS. Although we did see a dose-response effect, our results suggest that these two proteins are not ideal biomarkers for PFAA exposure in cetaceans due to the high sensitivity of the pathway in the range of doses tested. However, this does not lessen the concern for how these chemicals are disrupting this pathway in cetaceans, as higher doses induce expression similar to or greater than known positive controls.

This is the first *in vitro* study to investigate the potential of PPARα and CYP4A as biomarkers of PFAAs exposure in cetacean cells.

Introduction

Many endangered species of cetaceans are at high risk from anthropogenic stressors including environmental contamination. Perfluoroalkyl acids, PFAAs, are a class of persistent organic pollutants that have raised concern for marine mammal health. They are highly stable, man-made toxicants that have been produced since the 1950's and have since been investigated by the Environmental Protection Agency for concerns of their toxicity, ability to bioaccumulate, and persistence in the environment. While data suggests that perfluoroalkyl acids, PFAAs, have the potential to impact cetacean health severely, little is known about how these chemicals affect cetaceans at the cellular level.

The following evidence suggests that PFAA exposure poses a risk to marine mammals. It has been demonstrated that PFAAs have the ability to accumulate at high concentrations in marine mammals around the world (Houde et al., 2011). The ability for PFAAs to biomagnify within food webs increases the exposure risk for marine mammals and other organisms at high trophic levels (Kannan et al. 2004, Houde et al., 2006). Additionally, disease in sea otters is correlated with high concentrations of PFAAs. While this evidence supports the notion that PFAAs have the potential to cause serious health problems in cetaceans, very little is known about how these compounds affect marine mammal health on the cellular level.

Two studies have demonstrated a connection between PFAA exposure and the PPARα-CYP4A pathway, which is involved in the regulation of fatty acid metabolism. Ishibashi et al. (2008) found a positive correlation between perfluorononanoic acid, PFNA, levels and PPARα

expression in the livers of wild Baikal seals, as well as a significant correlation between CYP4A protein expression and PFNA and perfluorodecanoic acid, PFDA. Kurtz et al. (2014) established a correlation between PPARα mRNA and CYP4A protein expression and PFAA exposure in the kidneys of stranded cetaceans. This correlation suggests that the PPARα-CYP4A pathway is not only conserved in marine mammals, but may also be affected by PFAA exposure. The involvement of this pathway could cause serious health problems in marine mammals that rely on tightly regulated fatty acid catabolism for thermoregulation, stored energy, and oxygen conservation while diving (Trumble et al., 2012).

In order to establish that this cellular pathway is modified by the exposure to PFAAs and that another confounding factor is not responsible for the increased expression of PPARα-CYP4A seen in the wild marine mammals, a controlled experiment must be conducted in which the only variable is PFAA exposure. This will be accomplished by dosing a cell culture of *Tursiops truncatus* kidney cells with four concentrations of perfluorooctansufonic acid, PFOS, perfluorooctanoic acid, PFOA, perfluorononanoic acid, PFNA, and perfluorodecanoic acid, PFDA. Protein expression of PPARα and CYP4A was measured using western blotting to establish if protein expression increases with increasing PFAA dose.

Methods

Cell Culture:

The dolphin kidney cell line (DK1) was cultured and dosed with different concentrations of four PFAAs, PFDA, PFOS, PFNA, and PFOA. The cell line was maintained in a modified medium of Dulbecco's Modified Eagle's Medium (DMEM) to which fetal bovine serum (FBS)

10 ml/L and 100x penicillin-streptomycin-neomycin (PSN) were added. The final concentrations of FBS and PSN in the media were 10% and 0.1% respectively.

The media was changed every 2-4 days and the cells were grown until they reach 80-90% confluence. Once the desired confluence was reached the cells were passaged using 1 ml of Trypsin/EDTA to remove cells from the flask. Seeding concentration was determined using a hemocytometer and the dye Trypan blue to perform a cell count. Cells were passaged into either T-25 flasks or T-75 flasks and seeded at the respective densities of 0.7×10^6 and 2.1×10^6 determined by the cell count. All cells were maintained at 37°C, 95% humidity and 5% CO_2 until the dosing process was completed.

Once the cell count was high enough for the dosing procedure, the cells were removed from flasks using trypsin/EDTA. Cells were seeded in plates at suitable concentrations for cell confluence, 4.0×10^5 cells per well in 6 well plates and 2.0×10^4 cells per well in 96 well plates. The 96 well plates were used for the cell viability assay. Seeded cells were incubated for an additional 24 hours to adhere to the well plate. Cells were then dosed using the dosing procedure.

Dosing Procedure:

After the cells were incubated for 24 hours the following procedure was followed to dose the cells with the four PFAAs and controls at different concentrations. Each dosing solution contained DMEM, varying PFAA concentrations, and a vehicle used to dissolve the PFAA. Two different vehicles were used, DMSO and methanol. The vehicle used for PFOS was methanol with a final concentration of 0.38% (Meng et al., 2017, Shipley et al., 2004, Sundstrom et al., 2012, and Tanneberger et al.), because PFOS was not soluble in the concentration of DMSO (0.06%) used for the other chemical treatments. The vehicle used for the other three PFAAs,

PFDA, PFOA, and PFNA was DMSO with a final concentration of 0.06%. Cells were incubated for 24 hours in the medium containing the PFAA or the control.

The cells were dosed with the following three perfluorinated carboxylic acids: perfluorooctanoic acid (PFOA), perfluorononanoic acid (PFNA), perfluorodecanoic acid (PFDA). Only one perfluorinated sulfonic acid was used in cell dosing: perfluorooctane sulfonate (PFOS). The following three dosing concentrations were used for all PFAAs: 25 μM, 75 μM, and 225 μM. An environmentally relevant concentration was chosen for the lowest concentration and was as follows: PFOA 0.4 μM, PFOS 6 μM, PFDA 1 μM and PFNA 1 μM. Six replicates of each dose were conducted for each PFAA for a total of 96 dosed samples (Figure 2.2.).

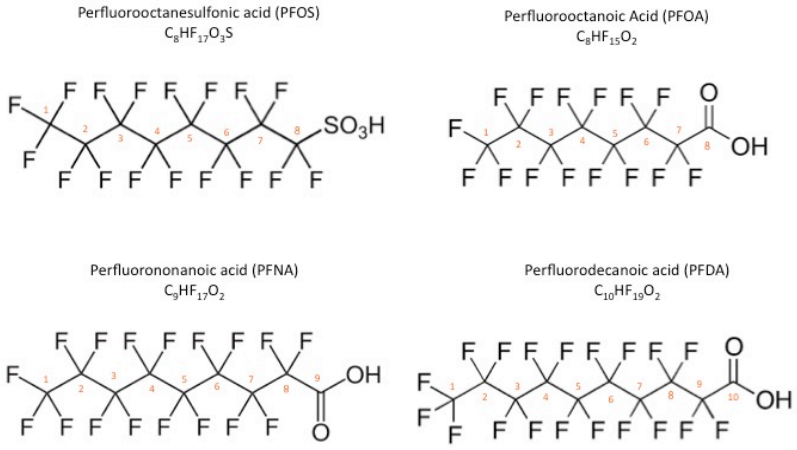

Figure 2.1. PFAA Structure of Chemicals Used in This Study
Chemical structure of PFOS, PFOA, PFNA and PFDA. Red numbers indicate carbon number.

In addition to dosing the cells with PFAAs, both positive and negative controls were used to exclude possible unknown factors that could be affecting cell viability or genetic expression of the different biomarkers. The positive controls were ligands known to induce expression of PPARα and CYP4A. The positive control used for PPARα was Wy-14,643 at concentrations of

10 µM and 20 µM (Rosen et al., 2008a; Shipley et al., 2004; Takacs & Abbott, 2007; Wolf et al., 2008). The positive control used for CYP4A was clofibric acid at concentrations of 100 µM and 200 µM (Parmentier et al., 1993). Positive controls were used to validate the PPARα-CYP4A pathway is conserved in the DK1 cell line.

Negative controls included cells that were not treated, and cells were treated with only a vehicle control. Untreated cells provided a baseline for cell expression of PPARα and CYP4A prior to cell dosing. Additionally, the vehicle control (treatment with DMSO or methanol) controlled for decreased cell viability or increased protein expression caused by the vehicle itself.

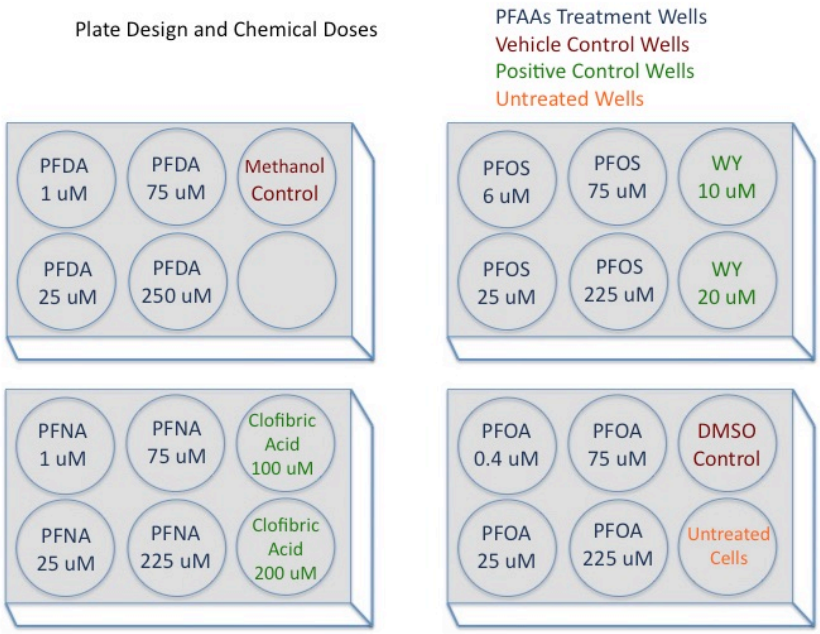

Figure 2.2. PFAA Dosing Scheme and Plate Design
Four PFAAs, PFNA, PFDA, PFOA, and PFOS were used to dose the cells. Four concentrations of each chemical were used. Positive controls included Wy-14,643, and clofibric acid. Negative controls are untreated cells. Vehicle controls included DMSO and Methanol. Six replicates of each treatment were performed.

Cell Viability Assay:

A cell viability assay was conducted using an EarlyTox™ Live/Dead Cell Viability Assay Kit and Molecular Devices FlexStation III. Calcein Am was used as a live-cell marker. In live cells Calcein Am is converted into calcein, which fluoresces green. EthD-III cannot enter live cells and was used as a dead-cell marker. When the membrane is compromised, EthD-III is able to enter the cell and bind to nucleic acids, and then fluoresces red. The microplate reader was then used to read the emitted fluorescence, which is measured as a Relative Fluorescence Unit (RFU). For each PFAA and control treatment, six replicates were performed. Cells were plated and dosed in 96-well black-sided plates with clear bottoms. Additional wells were used to calculate the background fluorescence of the media and the vehicle controls. Six wells contained media and DMSO and six wells contained media and methanol (Figure 2.3).

Live/Dead Assay Test:

	1	2	3	4	5	6	7	8	9	10	11	12
A												
B	DMSO	Methanol	C-100	C-200	WY-10	WY-20	PFOS6	PFOS25	PFOS75	PFOS225	NC MEOH	NC DMSO
C	DMSO	Methanol	C-100	C-200	WY-10	WY-20	PFOS6	PFOS25	PFOS75	PFOS225	NC MEOH	NC DMSO
D	DMSO	Methanol	C-100	C-200	WY-10	WY-20	PFOS6	PFOS25	PFOS75	PFOS225	NC MEOH	NC DMSO
E	DMSO	Methanol	C-100	C-200	WY-10	WY-20	PFOS6	PFOS25	PFOS75	PFOS225	NC MEOH	NC DMSO
F	DMSO	Methanol	C-100	C-200	WY-10	WY-20	PFOS6	PFOS25	PFOS75	PFOS225	NC MEOH	NC DMSO
G	DMSO	Methanol	C-100	C-200	WY-10	WY-20	PFOS6	PFOS25	PFOS75	PFOS225	NC MEOH	NC DMSO
H												

	1	2	3	4	5	6	7	8	9	10	11	12
A												
B	PFOA0.4	PFOA25	PFOA75	PFOA225	PFNA1	PFNA25	PFNA75	PFNA225	PFDA1	PFDA25	PFDA75	PFDA225
C	PFOA0.4	PFOA25	PFOA75	PFOA225	PFNA1	PFNA25	PFNA75	PFNA225	PFDA1	PFDA25	PFDA75	PFDA225
D	PFOA0.4	PFOA25	PFOA75	PFOA225	PFNA1	PFNA25	PFNA75	PFNA225	PFDA1	PFDA25	PFDA75	PFDA225
E	PFOA0.4	PFOA25	PFOA75	PFOA225	PFNA1	PFNA25	PFNA75	PFNA225	PFDA1	PFDA25	PFDA75	PFDA225
F	PFOA0.4	PFOA25	PFOA75	PFOA225	PFNA1	PFNA25	PFNA75	PFNA225	PFDA1	PFDA25	PFDA75	PFDA225
G	PFOA0.4	PFOA25	PFOA75	PFOA225	PFNA1	PFNA25	PFNA75	PFNA225	PFDA1	PFDA25	PFDA75	PFDA225
H												

Figure 2.3. Cell Viability Assay Design
The cell viability assay was designed to include all treatments and controls, as well as cells to calculate background fluorescence. C indicates clofibric acid, WY- indicates WY-14,643, numbers indicate the uM amount of each chemical used, and NC indicates wells that contained no cells, media and the vehicle controls to test for background fluorescence.

Protein Extraction:

The Invitrogen Trizol Reagent protocol was used to isolate the proteins (Appendix B). The concentration of protein in each sample was then quantified with a Nanodrop 2000 using

BCA colorimetric assay. An albumin standard was diluted in SDS to establish a standard curve, from which all protein concentrations were derived. The albumin standard and working reagent used were from a Pierce BCA Protein Assay Kit from Thermo Fisher Scientific.

Gel electrophoresis:

Once the protein fraction was isolated from the cells, the proteins were separated using gel electrophoresis. A miniVE electrophoresis unit (Hoefer, Inc.) was used to perform gel electrophoresis (Holliston, MA). The amount of protein solution needed to load 5 μg of protein in each well was calculated, so that each well contained an equal mass of protein. The protein solution was added to the appropriate amount of Pierce™ Lane Marker Reducing Sample Buffer. The samples were then denatured in boiling water for 3-5 minutes and placed on ice. A preformed 4-20% Tris-Glycine gels from NuSep, Inc. (Bogart, GA) in BupH™ Tris-Glycine-SDS was loaded with the samples, two lanes of the control with known protein expression and a ladder standard. To control for variation in imaging between gels, two different concentrations of the target protein were loaded into two of the wells. The control samples included: CYP4A from Sprague Dawley rat liver microsomes induced by clofibric acid from XenoTech, LLC (Lenexa, KS) and recombinant human PPARα protein from Novus Biologicals, LLC (Centennial, CO). These controls were used to determine the optical density ratio (ODR), which was the ratio of the optical density of the sample band to the optical density of the target protein control band. The unit was run at 200 volts for about one hour until the ladder reached the last 80-90% of the gel.

Western Blot Procedure:

After gel electrophoresis the gel was removed and the wells were cut and discarded from the gel. The protein transfer was then performed using an iBlot™2 transfer device with corresponding iBlot™2 transfer stacks. A nitrocellulose membrane was used to transfer the proteins. The transfer unit was layered correctly (Appendix A) and run at the R_0 preprogrammed setting (20 V for 1 min, 23 V for 4 min, and 25 V for 2 min).

After the transfer was complete the membrane was blocked using a blocking solution of 1:5 normal horse serum from Vector Laboratories to tris-buffered saline to reduce background signal and nonspecific binding of the antibodies. The membrane was blocked for one hour at room temperature on a shaker. Then the blot was washed four times with 30 ml of tris-buffered saline with 0.05% Tween-20 (TBST) for five minutes each wash. Primary antibodies and secondary antibodies were added to bind to the protein and as luminescent indicators. A reference protein, tubulin, was also targeted using antibodies and luminescent visualization to monitor for equal loading within each lane and to validate the condition of the sample.

The antibodies used were diluted in TBST in ratios of 1:1,500 of CYP4A primary antibody (catalogue # SC-271983 mouse CYP4A monoclonal antibody from Santa Cruz Biotechnology, Inc.), 1:1,500 of PPARα primary antibody (catalogue # MAB3890 mouse monoclonal anti-PPARα antibody from EMD Millipore), 1:5,000 of tubulin primary antibody (catalogue # DM1A of mouse monoclonal alpha tubulin primary antibody from Novus Biologicals), and 1:1,500 (CYP4A and PPARα) and 1:1,000 (alpha tubulin) of secondary antibody (catalogue # 32430 goat anti-mouse IgG peroxidase conjugated from Thermo Fisher Scientific). The blots were incubated with the primary antibody overnight at 5˚C, and then for one hour on a shaker at room temperature. Between primary and secondary antibodies and after the secondary antibody incubation, the blot was washed four times with 30 ml TBST for five

minutes each wash. The blot was incubated in the secondary antibody for two hours at room temperature on an orbital shaker. After the blot was imaged to detect for PPARα or CYP4A the blot was stripped using Reblot Plus Strong Stripping Solution 10x from EMD Millipore. The blot was then probed for tubulin using the same procedure for antibody incubation and washing.

Chemiluminescent visualization and band density quantification was performed using WesternSure™ Premium Substrate, a C-DiGit Blot Scanner, and Image Studio software (version 4.0.21) from LI-COR, Inc. (Lincoln, NE). Recommended incubation times of 5 minutes were used in the LI-COR substrate, and the blots were scanned using the high intensity setting on the Image Studio software. The intensity of the protein signal was read to quantify the amount of protein in each sample.

Statistical Analysis:

Statistical analyses were performed using JMP® version 14 from SAS to determine if protein expression was significantly different in cells treated with PFAAs compared to the vehicle control. The data did not follow a normal distribution, so the non-parametric Kruskal-Wallis one-way analysis of variance was used to compare means. For significant values, multiple non-parametric comparisons were conducted using the Wilcoxon Signed-Rank Test. Alpha was set to 0.05. Outliers were identified using a Tukey outlier box plot and removed from the dataset.

Results and Discussion

Cell Viability Assay and Visual Observations:

The following cell treatments had the highest number of dead cells: PFOA 0.4 μM (15.4 RFU), PFOA 75 μM (23.5 RFU), PFNA 225 μM (19.6 RFU), PFDA 75 μM (21.8 RFU) and

PFDA 225 µM (16.3 RFU) (Figure 2.5.). When dead cells were measured, cell death did not correspond with increased concentration for any chemical. However, the ratio of live to dead cells indicated that cell viability decreased with increasing dose (Figure 2.5.). The lack of agreement between the live to dead ratio and the dead cell measurement indicates that the higher chemical concentrations not only increased cell death, but also suppressed cell proliferation.

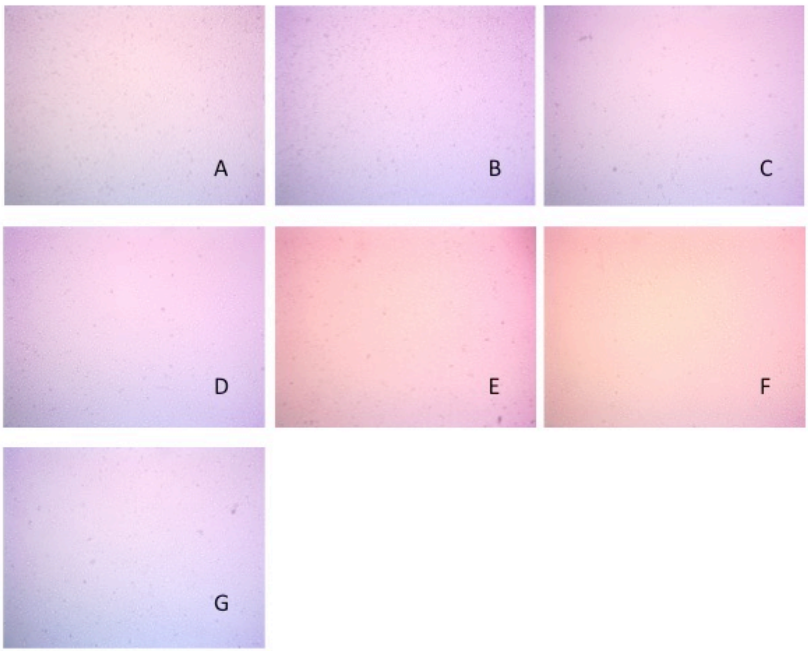

Figure 2.4. Pictures of cells dosed with control chemicals
A.) No Treatment B.) Methanol C.) Wy 10 µM D.) Wy 20 µM E.) Clofibric Acid 100 µM F.) Clofibric Acid 200 µM G.) DMSO. Pictures were taken at 4x using an AmScope MU1000A MP Still and Live Microscope Digital Camera. Cells treated with control chemicals appeared healthy. Untreated cells were 100% confluent.

Cell viability was lowest, indicated by the lowest values for the ratio of live to dead cells, for the following treatments: PFOS 225 µM (43.2), PFNA 225 µM (24.2), PFDA 75 µM (12.1) and PFDA 225 µM (3.12) (Figure 2.5.). The highest cell viability, indicated by the highest values for the ratio of live cells to dead cells were PFOA 25 µM (90.1), PFDA 1 µM (100.4), PFNA 1µM (102.7), and PFNA 25 µM (130.9). For all chemicals except PFOA, cell viability was lower for the highest dose of PFAA than the vehicle control. Although cell viability decreased with

increasing dose of PFOA, the ratio of live to dead cells was greater than the vehicle control, DMSO (55.1, 67.8 respectively). Thus all concentrations of PFOA had less of a negative effect on cell viability than the vehicle alone.

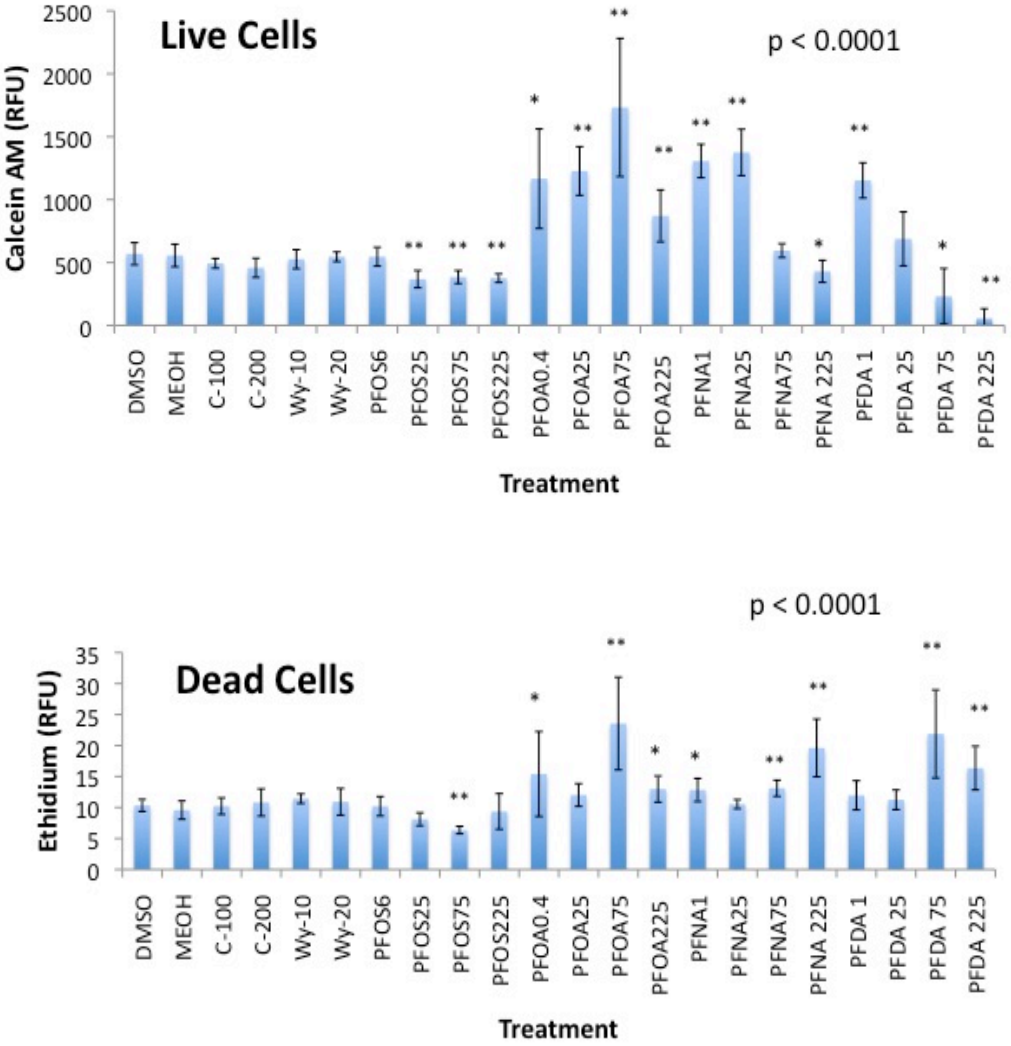

Figure 2.5. Cell Viability Assay Live and Dead Cells
A cell viability assay was conducted with an Early Tox Live/Dead Assay Kit from Molecular Devices and a fluorescence microplate reader. Calcein Am was used as a live cell marker. Live cells convert Calcein AM into calcein which fluoresces green. Ethidium D was used as a dead cell marker, indicating dead cells by the intensity of red fluorescence. The relative fluorescence units (RFU) were measured. Error bars indicate one standard deviation. * indicates treatments that were significantly different from the vehicle control (*$p < 0.05$, ** $p < 0.01$). n = 6.

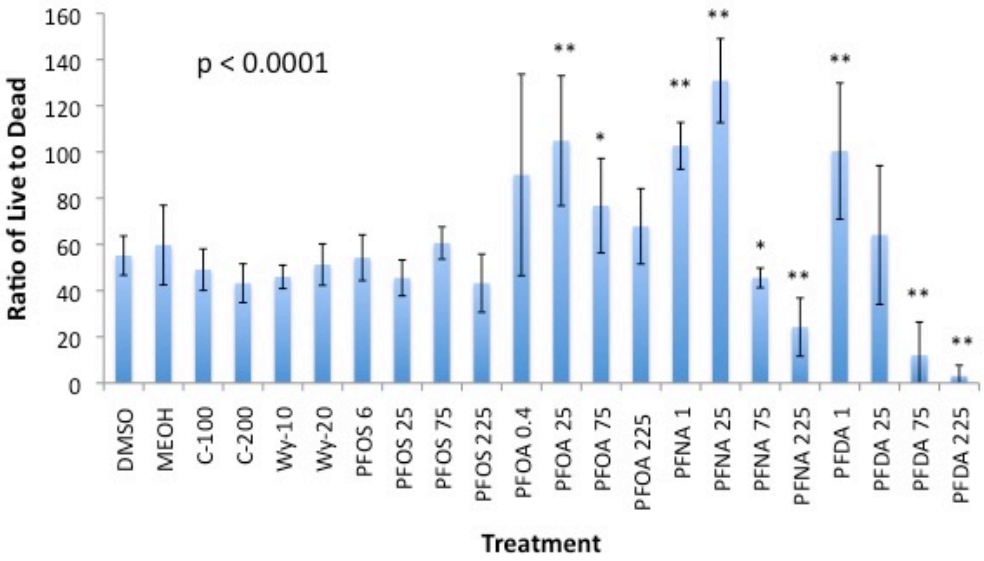

Figure 2.6. Cell Viability Assay Ratio of Live to Dead Cells
The ratio of live to dead cells was calculated from the cell viability assay conducted with an Early Tox Live/Dead Assay Kit from Molecular Devices. A microplate reader measured the relative fluorescence units (RFU) of both live and dead cells. Calcein Am was used as a live cell marker and fluoresces green in live cells. Ethidium D was used as a dead cell marker and fluoresces red in dead cells. Error bars show one standard deviation. * indicates treatments that were significantly different from the vehicle control (*$p < 0.05$, **$p < 0.01$,). $n = 6$.

Visual observations support the results of the cell viability assay. Cells appeared confluent at the center of each well, although cell confluence around the edges of the wells was diminished with the exception of untreated cells. In untreated wells, cell confluence was 100% (Figure 2.4.). In treated wells, cell confluence was 100% at the center and 80-100% at the edge, except for the higher concentrations of PFOS where cell confluence at the outermost edge appeared to be only 50-60% (Figure 2.4. and 2.7-2.10.).

Although cells treated with the 225 µM of PFOS appeared to be only 50-60% confluent around the edges of the well, there was less of a decrease in cell viability for the highest concentration of PFOS than PFDA and PFNA; the ratios of live to dead cells were 43.2, 3.12, and 24.2 respectively. While the observed confluence of the cells suggests cell viability should also be low, there were fewer dead cells in wells treated with PFOS than other treatments, which

increased the cell viability. The decrease in cell confluence around the edge of the well for cells treated with 225 µM PFOS is consistent with the low value obtained for live cells at this concentration (375.58 RFU). Additionally, dead cells were observed and recorded in wells treated with 225 µM of PFOS (Figure 2.7); however, a relatively low number of dead cells were measured (9.36 RFU). Therefore, cell proliferation was highly repressed by the highest concentration of PFOS, and fewer cells died from this treatment than PFDA or PFNA.

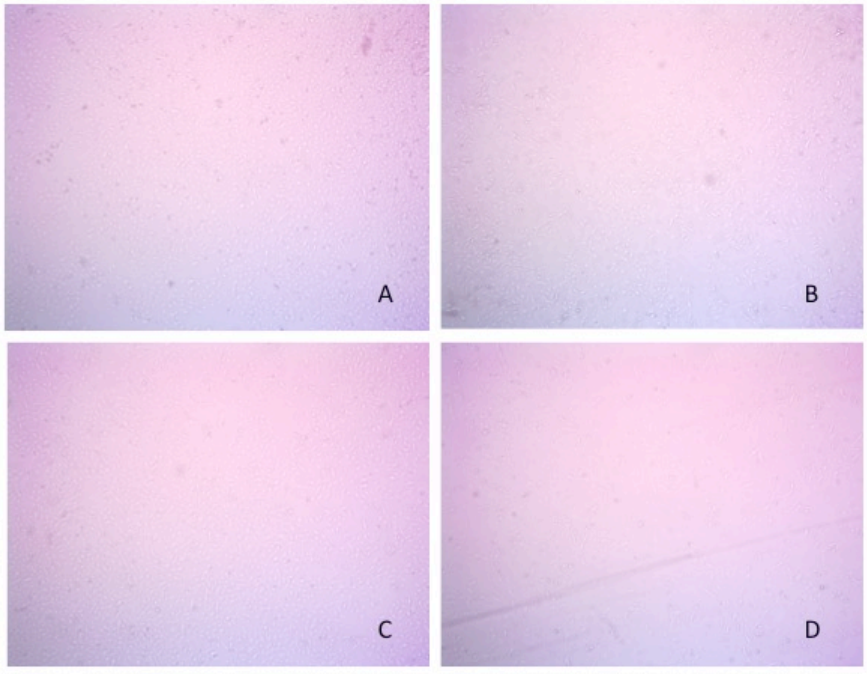

Figure 2.7. Pictures of cells dosed with PFOS
A.) 6 µM B.) 25 µM C.) 75 µM D.) 225 µM. Pictures were taken at 4x using an AmScope MU1000A MP Still and Live Microscope Digital Camera. There was a decrease in cell confluence at higher doses, C and D.

The two highest concentrations of PFDA (75 µM and 225 µM) induced the lowest cell viability, indicated by the lowest ratios of live to dead cells. The cells in these wells were misshapen and less confluent than the other cells treated with PFDA as seen in Figure 2.8. Instead of appearing to be adhered to the bottom of the well and elongated, the cells appeared

round and spherical. The misshapen cells did not appear to be dead. There was a clear difference between misshapen cells and cells that were assumed to be dead, which were also spherical in shape but were floating instead of being adhered to the plate. Dead cells were recorded floating in the cell media at the two highest concentrations of PFDA, 75 µM and 225 µM. These observations were consistent with high numbers of dead cells measured in these two treatment wells (21.88 RFU and 16.36 RFU respectively).

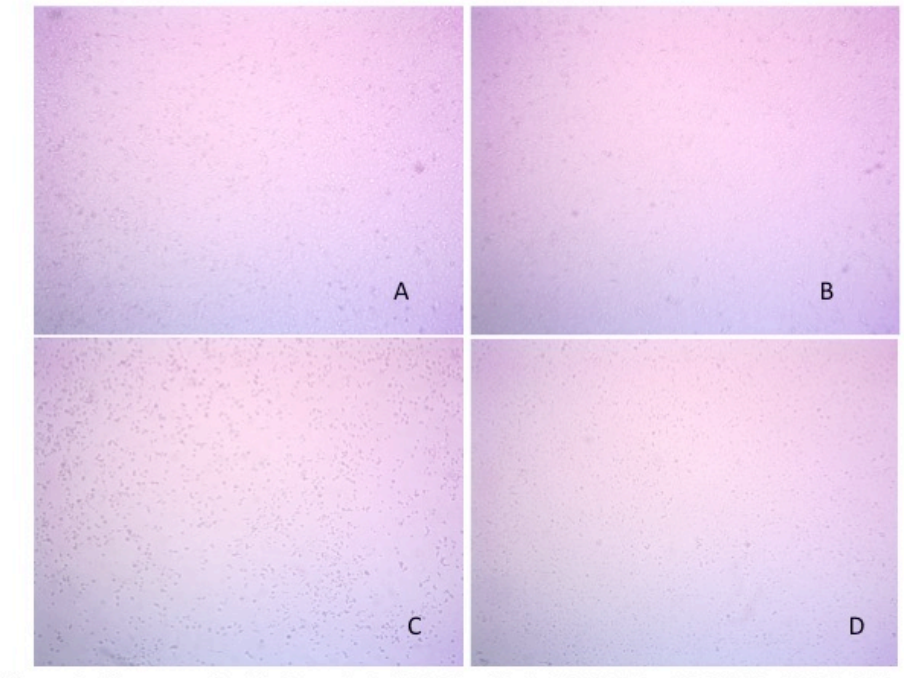

Figure 2.8. Pictures of cells dosed with PFDA
A.) 1 µM B.) 25 µM C.) 75 µM D.) 225 µM. Pictures were taken at 4x using an AmScope MU1000A MP Still and Live Microscope Digital Camera. There was a decrease in cell confluence at higher doses, C and D. Additionally there was a change in cell shape at higher doses, C and D.

Of all treatments, including controls, PFNA had the highest ratio of live to dead cells at the 25 µM dose (130.9), indicating the greatest cell viability (Figure 2.6.). There was a drastic decrease in cell viability at the two highest doses 75 µM and 225 µM (45.5 and 24.2

respectively). Dead cells were observed floating in the media at the highest concentration, 225 µM (Figure 2.7.). While the number of dead cells did increase at these concentrations, the number of live cells drastically decreased (Figure 2.5.), suggesting that the change in cell viability was due more to a decrease in cell proliferation. Cells also appeared to be misshapen at the 225 µM dose of PFNA; although, the change in shape was not as apparent as PFDA at the same concentration.

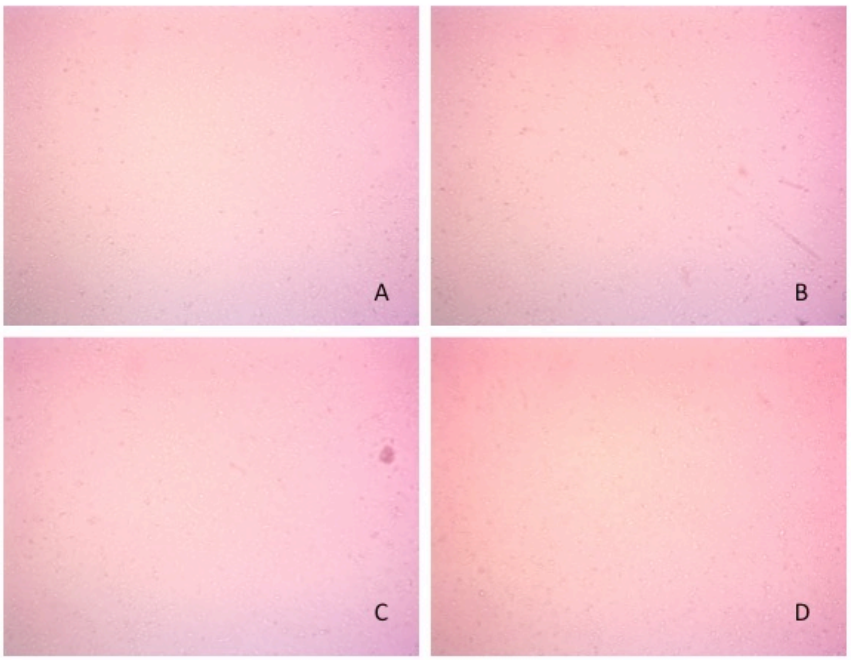

Figure 2.9. Pictures of cells dosed with PFNA
A.) 1 µM B.) 25 µM C.) 75 µM D.) 225 µM. Pictures were taken at 4x using an AmScope MU1000A MP Still and Live Microscope Digital Camera. There was a decrease in cell confluence at higher doses and a change in cell shape, C and D.

The wells treated with the highest dose of PFOA appeared to be the most confluent out of all the high chemical doses (Figure 2.10.). This was supported by the ratio of live to dead cells. PFOA 225 µM had the highest live to dead ratio for cells treated with 225 µM (67.8). Additionally, for each treatment of PFOA the number of live cells was significantly greater than the vehicle control. Therefore, cell proliferation was induced by PFOA. Other studies have

suggested PFOA can stimulate cell proliferation, and can be one of the reasons tumors occur with exposure (Olsen et al., 2003 and Klaunig et al., 2012). Conversely, in rat thymocytes and splenocytes, cell proliferation decreased with PFOA exposure (Yang et al., 2001). This suggests that PFOA has an effect on the regulation of cell cycle. While cell proliferation was the highest in cells treated with PFOA, there was still a decrease in the ratio of live to dead cells at increasing dose. The second highest dose of PFOA, 75 µM, had the highest number of dead cells measured (23.5 RFU). This suggests that cell death, not proliferation, influences cell viability with PFOA treatment.

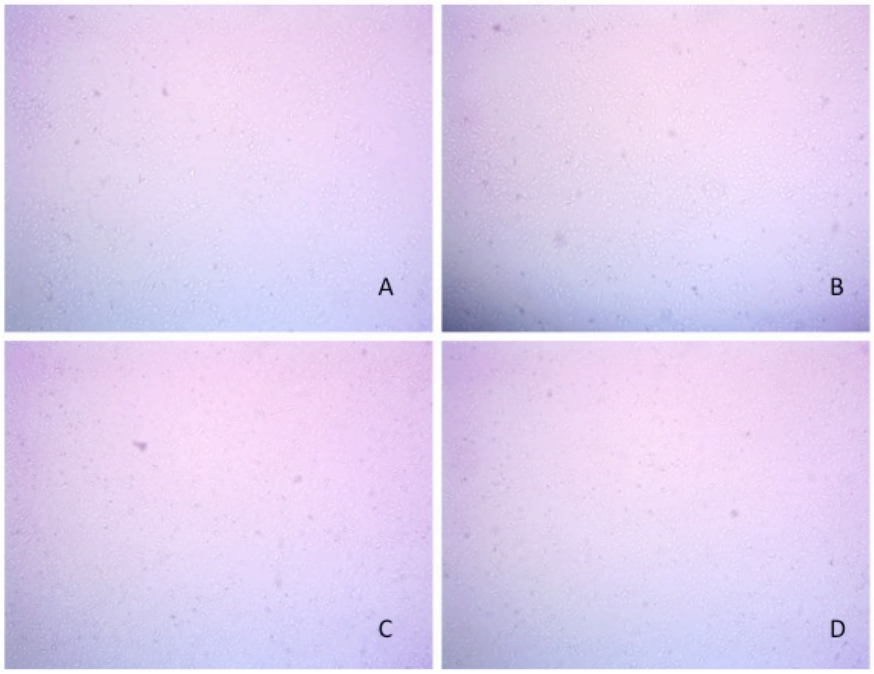

Figure 2.10. Pictures of cells dosed with PFOA
A.) 0.4 µM B.) 25 µM C.) 75 µM D.) 225 µM. Pictures were taken at 4x using an AmScope MU1000A MP Still and Live Microscope Digital Camera. There was a decrease in cell confluence at the highest dose, D.

Positive Controls

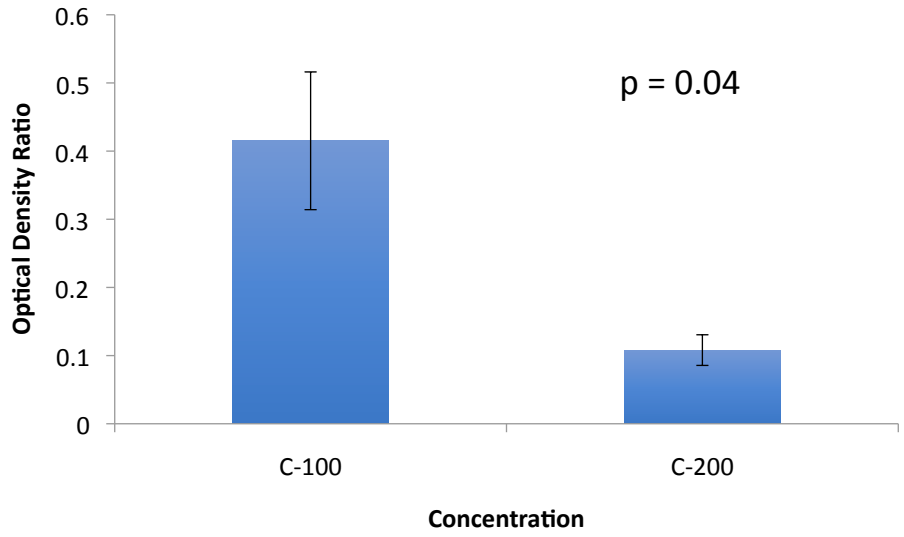

Figure 2.11. CYP4A expression of cells dosed with clofibric acid
Dolphin kidney cells were treated with clofibric acid (100 µM and 200 µM). The data show the mean ± SE. p = 0.04. The optical density ratio is the ratio of the optical density of the sample to the optical density of an internal control standard of cytochrome P4504A from rat liver microsomes, XenoTech LLC product R1063. n = 5 to 6.

Both concentrations of the positive control, clofibric acid, induced a greater expression of CYP4A than the blank and vehicle control (Figure 2.11.). The expression of CYP4A induced by the lower concentration of clofibric acid (100 µM) was four times greater than the higher concentration (200 µM), Figure 2.11. The difference in expression was statistically significant (p = 0.0446). The same pattern was seen in the positive control Wy-14,643 used to induce PPARα (Figure 2.12.). The higher concentration (20 µM) of Wy-14,643 induced six fold lower expression than lower concentration (10 µM), Figure 2.12. The difference in expression was statistically significant (p = 0.0285). Additionally, there was less PPARα induction by higher concentration of WY-14,643 than the untreated cells (mean = 0.0563 ODR and 0.101 ODR respectively). This decrease in expression at the higher concentration could suggest that there is a threshold concentration that induces the highest expression of PPARα and CYP4A, and that

concentrations higher than this threshold are reducing the activity of this pathway. Additionally, it suggests that this pathway is very sensitive to small changes in concentrations, and it is easy to exceed this threshold of expression.

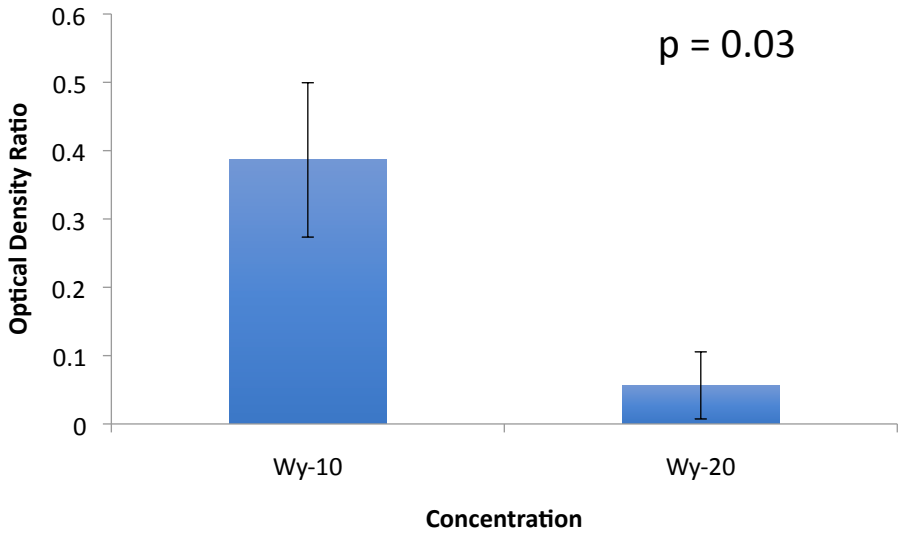

Figure 2.12. PPARα expression of cells dosed with Wy-14,643
Dolphin kidney cells were treated with Wy-14,643 (10 µM and 20 µM). The data show the mean ± SE. p = 0.03. The optical density ratio is the ratio of the optical density of the sample to the optical density of an internal control standard of recombinant human PPARα protein from Novus Biologicals. n = 5 to 6.

Vehicle Controls

There was no statistical difference ($p < 0.05$) between the DMSO vehicle control and the non-treatment cells for both PPARα expression and CYP4A expression (Figure 2.14 and Figure 2.18.). Therefore, DMSO at this concentration (0.06%) was an appropriate vehicle for diluting the PFAAs into the cell media. Statistical comparisons were drawn between the DMSO vehicle control and the dose concentrations.

In contrast, there was a significant difference ($p < 0.05$) between the expression of CYP4A in the methanol treated cells and the non-treatment cells, Figure 2.13. Thus, 0.38% of methanol in the cell media was not an appropriate vehicle. The response in CYP4A expression induced by methanol was almost 10-fold higher than the expression in cells treated only with media ($p = 0.0163$). Additionally, the expression of CYP4A in the methanol treatment (mean = 0.590 ODR) exceeded the expression induced by the positive control, 100 µM clofibric acid (mean = 0.415 ODR).

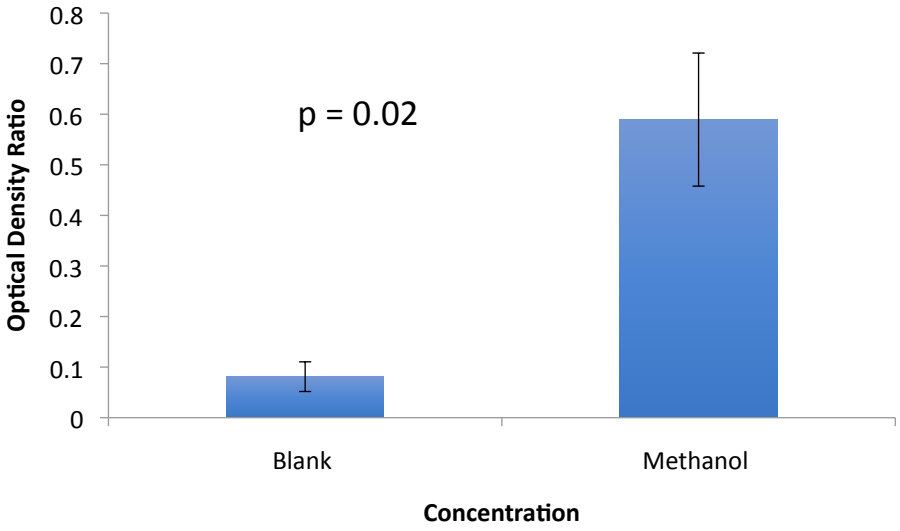

Figure 2.13. CYP4A expression in untreated cells and cells treated with methanol as a vehicle control
Dolphin kidney cells were treated with methanol (vehicle control). Blank indicates untreated cells. The data show the mean ± SE. $p = 0.02$. The optical density ratio is the ratio of the optical density of the sample to the optical density of an internal control standard of Cytochrome P4504A from rat liver microsomes, XenoTech LLC product R1063. $n = 5$.

One possible explanation was the concentration of methanol used, which was much higher than the concentration of DMSO used. The final concentration of DMSO in the media was 0.06% while the final concentration of methanol in the media was 0.38%. Methanol has been documented to have an effect on CYP1A, CYP2C, CYP2D, CYP2E and, CYP3A-mediated

metabolism in rat liver microsomes (Li et al., 2010); however, the effects occurred at concentrations greater than 1%. Additionally, DMSO was shown to change CYP activity at even lower concentrations than methanol (< 1%) (Li et al., 2010). Therefore, the concentration of 0.38% was not expected to induce CYP4A expression, which could indicate the DK1 cells may be more responsive to methanol compared to other cell lines. Methanol has been documented to increase CYP activity in fruit flies (CYP318A1, CYP4E2, CYP4D2, CYP6W1, CYP4AA1, CYP304A1, CYP28A5 and CYP30A1), humans (CYP2C8/9 and CYP2E1), rodents (CYP2D, CYP 2E1), and zebra fish larvae (CYP1, CYP2 and CYP3) (Wang et al., 2013, Chauret et al., 2019, Allis et al. 1996, Li et al., 2010 and David et al., 2012). Since methanol induced CYP4A activity, cell treatment groups were compared to both the vehicle control and the non-treatment cells for PFOS for statistical significance.

CYP4A Protein Expression

CYP4A Expression with Exposure to PFNA

In cells treated with PFNA, the expression of CYP4A followed a biphasic dose dependent expression pattern. The expression of CYP4A increased with increasing PFNA concentration up to 75 μM, and then decreased at the highest dose of 225 μM (Figure 2.14.). Additionally, the expression of CYP4A was greater in both the vehicle control and untreated cells than the two lowest concentrations (1 μM and 25 μM) and the highest concentration (250 μM). Only one concentration, 75 μM, induced an expression of CYP4A that was greater than the untreated cells and the vehicle control. Even the highest expression of CYP4A in PFNA treated cells (75 μM) was four times lower than the expression in cells treated with 100 μM of the positive control, clofibric acid. However, the difference between the vehicle control and CYP4A expression in

dosed cells was not significant (p = 0.1809).

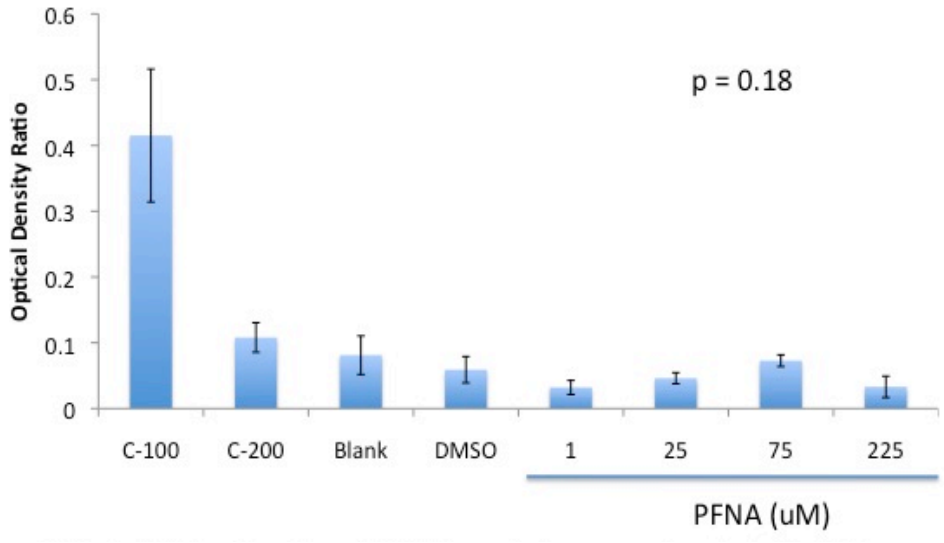

Figure 2.14. PFNA activation of CYP4A protein expression

Dolphin kidney cells were treated with clofibric acid (100 µM and 200 µM), DMSO (vehicle control), and PFNA at the concentrations indicated. Blank indicates untreated cells. The data show the mean ± SE. The optical density ratio is the ratio of the optical density of the sample to the optical density of an internal control standard of Cytochrome P4504A from rat liver microsomes, XenoTech LLC product R1063. n = 4 to 6

CYP4A Expression with Exposure to PFOA

While there was a dose dependent relationship in CYP4A expression with exposure to PFOA, the expression of CYP4A deviated from the other chemicals tested and decreased with increasing PFOA dose (Figure 2.15.). The greatest expression was seen at the lowest dose, 0.4 µM, and was almost 4-fold greater than the expression in the vehicle control, DMSO, cells (mean = 0.226 ODR and 0.0591 ODR respectively). All four concentrations induced greater expression than the DMSO vehicle control (mean = 0.0591 ODR) and the higher concentration of the positive control, 200 µM clofibric acid (mean = 0.108 ODR). However, there was no

significant difference between PFOA treated cells and the vehicle control (p = 0.7996).

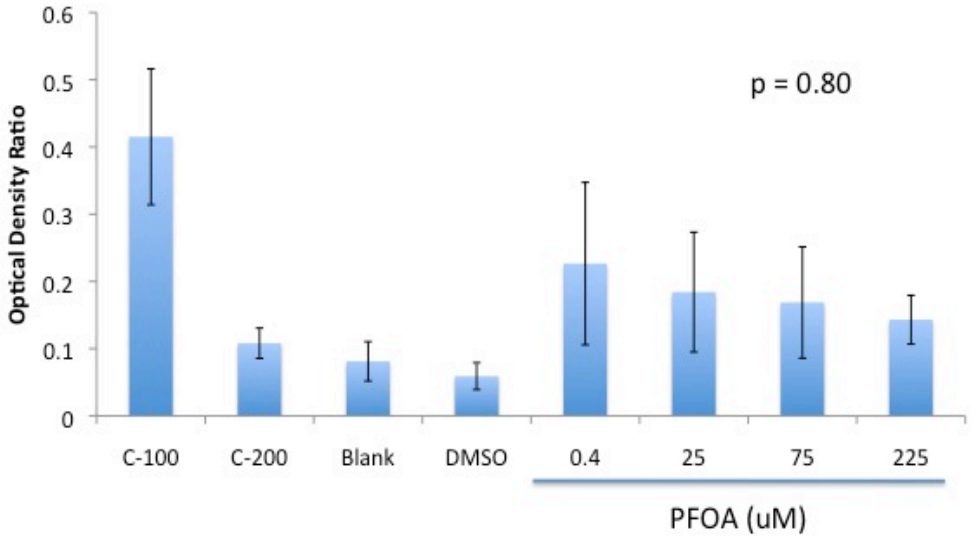

Figure 2.15. PF0A activation of CYP4A protein expression
Dolphin kidney cells were treated with clofibric acid (100 µM and 200 µM), DMSO (vehicle control), and PFOA at the concentrations indicated. Blank indicates untreated cells. The data show the mean ± SE. The optical density ratio is the ratio of the optical density of the sample to the optical density of an internal control standard of cytochrome P450 from rat liver microsomes, XenoTech LLC product R1063. n = 6.

CYP4A Expression with Exposure to PFOS

A dose-response was seen in PFOS treated cells; CYP4A expression increased with increasing dose of PFOS (Figure 2.16.). There was a significant difference between expression induced by the methanol control and by all four concentrations of PFOS (p = 0.0013). However, this significant difference was driven by the induction of CYP4A by the methanol vehicle. Methanol was deemed to be an inappropriate vehicle, therefore the results of the dosed cells are not conclusive. However, the 225 µM dose was statistically different from the 6 µM and 25 µM treatment. This could suggest that with an appropriate vehicle, a significant pattern of induction could be measured.

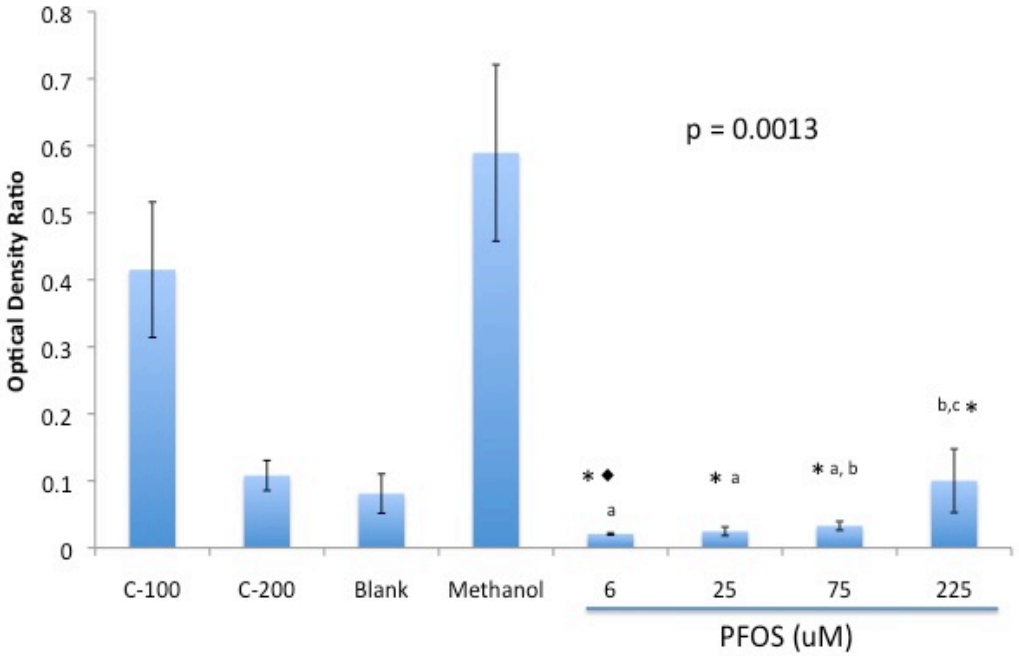

Figure 2.16. PF0S activation of CYP4A protein expression
Dolphin kidney cells were treated with clofibric acid (100 µM and 200 µM), Methanol (vehicle control), and PFOS at the concentrations indicated. Blank indicates untreated cells. The data show the mean ± SE. The optical density ratio is the ratio of the optical density of the sample to the optical density of an internal control standard of cytochrome P450 from rat liver microsomes, XenoTech LLC product R1063.* indicates a significant difference in CYP4A protein expression in the PFAA treated cells from the vehicle control, methanol. ♦ indicates a significant difference in CYP4A protein expression in PFAA treated cells from the untreated cells. Bars with the same letter indicate values that are not statistically different from each other ($p < 0.05$). n = 5 to 6.

CYP4A expression only exceeded the untreated cells at the highest concentration of PFOS, 225 µM (mean= 0.0811 ODR and 0.102 respectively ODR). Additionally, all four-treatment concentrations were significantly lower than the methanol control. Even the smallest concentration completely negated the expression induced by methanol as a vehicle. Therefore, the addition of PFOS to the cells may have had such a detrimental effect on the cells that the pathway is no longer able to function at the same capacity. The expression induced by the lowest concentration, 6 µM, was three fold lower than the expression seen in untreated cells (mean = 0.021 ODR and 0.811 respectively ODR). The lowest concentration of clofibric acid, 100 µM,

induced four-fold greater expression than the highest concentration of PFOS, 225 µM (mean= 0.415 ODR and 0.102 ODR respectively). Therefore, while CYP4A expression increased with increasing dose, the effects of PFOS on the cell may completely dampen the expression of CYP4A induced by methanol. Another study with an appropriate vehicle would need to be completed to verify these results. Three outliers were removed from the data set, Table 2.1.

Table 2.1. Optical Density Ratio of CYP4

	Optical Density Ratio (Relpicates 1-6)					
Chemical Dose (uM)	1	2	3	4	5	6
PFOS 6	0.0274	0.0201	0.0180	0.8000	0.0181	0.0213
PFOS 25	0.0452	0.0329	0.0230	0.3258	0.0118	0.0112
PFOS 75	0.0536	0.0405	0.0300	0.2515	0.0146	0.0260
PFOS 225	0.0367	0.0633	0.0448	0.3311	0.0258	0.0998
PFOA 0.4	0.0698	0.0039	0.0091	0.0811	0.4967	0.6982
PFOA 25	0.1220	0.0263	0.0097	0.0881	0.5870	0.2715
PFOA 75	0.1078	0.0612	0.0080	0.0874	0.5655	0.1822
PFOA 225	0.1579	0.0495	0.0483	0.1159	0.2623	0.2245
PFDA 1	0.0590	0.9387	0.4332	0.5295	0.0436	0.0452
PFDA 25	0.1556	0.7068	0.6947	0.1771	0.0274	
PFDA 75	0.8996	0.6874	0.1476	0.0217		
PFDA 225	1.0426	0.6390	0.1581			
PFNA 1	0.0251	0.0695	0.0238	0.0050	0.0370	
PFNA 25	0.0678	0.0609	0.0471	0.0241	0.0305	
PFNA 75	0.0995	0.0690	0.0752	0.0764	0.0436	
PFNA 225	0.0781	0.0248	0.0287	0.0006		

[a] The Optical Density Ratio is the ratio of the optical density of the sample to the optical density of an internal control standard of Cytochrome P450 from rat liver microsomes, XenoTech LLC product R1063. Optical Density values were determined through Western blot. Red values indicate outliers that were removed from the data set.

Table 2.2 Optical Density Ratio of PPARα

	Optical Density Ratio (Relpicates 1-6)					
Chemical Dose (uM)	1	2	3	4	5	6
PFOS 6	0.6255	1.1148	0.0262	0.0043	0.0032	0.0158
PFOS 25	0.5883	1.3925	0.0155	0.0008	0.0002	0.0171
PFOS 75	0.4897	3.1350	0.0243	0.0015	0.0004	0.0203
PFOS 225	0.4488	5.2984	0.0165	0.0080	0.0005	0.0500
PFOA 1	0.3763	0.3867	0.8039	0.2792	0.3960	0.9040
PFOA 25	0.5692	0.0830	0.2357	0.5356	0.1208	0.9046
PFOA 75	0.2490	0.0822	0.9245	0.0938	0.1776	0.9750
PFOA 225	0.1176	0.0967	0.5211	0.7926	0.2876	1.4871
PFDA 1	1.2433	0.2146	0.3568	0.0948	0.0238	
PFDA 25	0.7521	0.1608	0.0672	0.0588		
PFDA 75	0.6977	0.0834	0.0310	0.0169	0.0832	
PFDA 225	0.2896	0.0638	0.0522			
PFNA 1	0.0437	0.0053	0.0053	0.0308	0.0370	1.1572
PFNA 25	0.0403	0.0347	0.0030	0.0117	0.0335	0.4816
PFNA 75	0.1983	0.0277	0.0468	0.0107	0.0440	0.3141
PFNA 225	0.2779	0.0699	0.2710	1.2986		

[a] The Optical Density Ratio is the ratio of the optical density of the sample to the optical density of an internal control standard of recombinant human PPAR alpha protein from Novus Biologicals. Optical density values were determined through Western blot. Red values indicate outliers that were removed from the data set.

CYP4A Expression with Exposure to PFDA

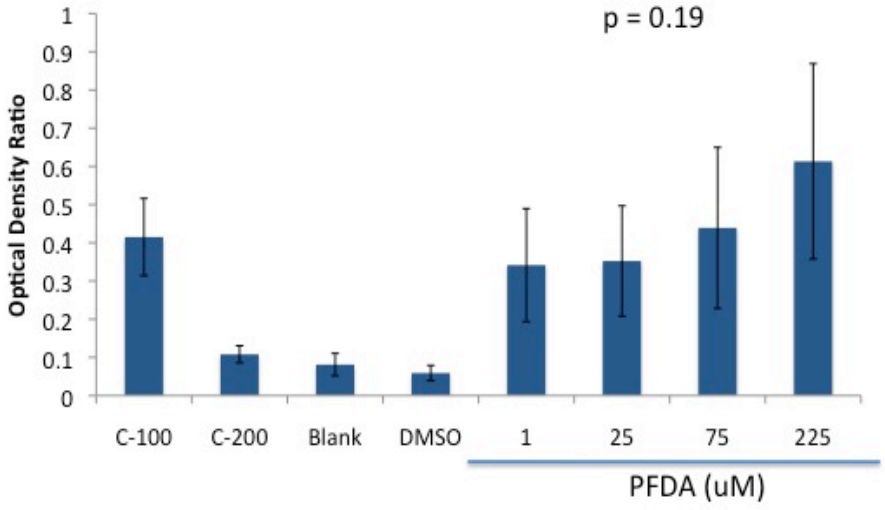

Figure 2.17. PFDA activation of CYP4A protein expression
Dolphin kidney cells were treated with clofibric acid (100 µM and 200 µM), DMSO (vehicle control), and PFDA at the concentrations indicated. Blank indicates untreated cells. The data show the mean ± SE. The optical density ratio is the ratio of the optical density of the sample to the optical density of an internal control standard of Cytochrome P450 from rat liver microsomes, XenoTech LLC product R1063. n = 3 to 6.

With increasing concentration of PFDA, there was an increase in CYP4A expression (Figure 2.17.). CYP4A protein expression was higher than the 100 µM clofibric acid positive control (mean = 0.415 ODR) in both of the two highest PFDA concentrations, 75 µM (mean = 0.439 ODR) and 225 µM (mean = 0.613 ODR). The expression induced by the lowest concentration, 1 µM, (mean = 0.342 ODR) was 5-fold greater than the DMSO vehicle control (mean = 0.0591 ODR). The expression induced by highest concentration of PFDA, 225 µM, (mean = 0.613 ODR) was 10 fold greater than the vehicle control. However, there was no significant difference between the PFDA treatment groups and the vehicle control ($p = 0.1907$).

Relationship Between PFAA Structure and CYP4A Expression

The trend of carboxylates inducing higher activity of expression than sulfonates (Wolf et al., 2008) was observed in these treated cells. The highest expression induced by 0.4 μM PFOA (mean = 0.226 ODR) was greater than the highest expression induced by 225 μM PFOS (mean = 0.102 ODR). Although, this trend was complicated by pattern of expression seen with exposure to these two chemicals. CYP4A expression with increasing concentration of PFOA decreased while CYP4A expression with increasing concentration of PFOS increased. While the optical density ratio measured for the highest concentration of PFOA (mean = 0.143 ODR) still exceeded the optical density ratio measured for PFOS at this concentration (mean =0.102 ODR), it is unknown if CYP4A expression induced by wider concentration range of these chemicals would maintain the same pattern. Testing a wider range of concentrations would help elucidate this pattern.

Other studies have shown a relationship between carbon chain length and PPARα expression with increased expression up to eight carbons; and it was hypothesized that CYP4A would follow the same expression pattern. However, the relationship between PFAA carbon chain length and CYP4A expression was convoluted by high expression seen in cells treated PFDA. Markedly higher expression of CYP4A was seen in cells treated with PFDA (10 carbons) than PFNA (9 carbons). The expression induced by highest concentration of PFDA, 225 μM, (mean = 0.613 ODR) was 10 fold greater than the 100 μM vehicle control (mean = 0.415 ODR). In contrast, the expression induced by 225 μM of PFNA (mean = 0.0728 ODR) was four fold lower than the expression in the 100 μM vehicle control. Suggesting that the trend of increasing expression with carbon length up to eight carbons does not hold true for these cells. However, the lowest expression induced by PFOA (8 carbons) was greater than the highest expression of

PFNA (9 carbons). The mean optical density ratio for 225 μM of PFOA was 0.143 and the mean optical density ratio for 225 μM PFNA was 0.0728. This supports the hypothesis that PFAAs with carbon chain lengths greater than 8 do not induce higher expression. This could possibly indicate a species-specific difference in the activation potential PFNA. Species-specific differences have previously been identified for PFOA. Rosen et al., (2013) found that PFOA induced less activity in human hepatocytes than in mouse hepatocytes. In this study, only a small range of carbon chain lengths were tested. To fully understand the relationship between carbon chain length and CYP4A expression in these cells more PFAAs of varying chain lengths should be tested.

CYP4A as a Biomarker

Of the four PFAAs tested in this study, Kurtz et al. (2019) found CYP4A expression to only be correlated with PFDA concentration in the kidney, when single compounds were evaluated alone. Additionally, Ishibashi et al., (2008) found a correlation between PFNA and PFDA concentration and CYP4A like protein in the liver of Baikal seals. These results could corroborate Kurtz et al.'s (2019) and Ishibashi et al.'s (2008) findings, because the expression of CYP4A induced by PFDA was greater than any of the other four chemicals tested. Therefore, PFDA may have a great enough impact on CYP4A expression to elicit a measurable change in CYP4A concentration in live animals even though the change in expression in these cells was not significant. The response for PFNA; however, showed a considerably lower fold change in expression of CYP4A. Suggesting that the same pattern of CYP4A expression may not be seen in cetaceans exposed to PFNA as Baikal seals. This supports Kurtz et al.'s (2019) findings that there was no correlation between PFNA and CYP4A expression in cetaceans.

On the other hand, an alternative interpretation could explain the patterns seen in the CYP4A expression induced by PFOA, PFNA and PFOS that could corroborate Kurtz et al.'s findings. Kurtz et al., (2019) did not find a correlation between these three chemicals and CYP4A protein expression in the kidney tissues of cetaceans stranded in Hawaiian waters. The change in expression of CYP4A in cells treated with PFOA was not significant, which could indicate that PFOA does not induce CYP4A in cetacean cells. However, a lack of significant increase in CYP4A expression could also indicate that the lowest dose of PFOA, a concentration found in exposed animals, has already exceeded the threshold of toxic injury in these cells. Toxic injury in the cell is suggested by the decrease in cell viability with increasing PFOA concentration.

Additionally, increased sensitivity of the PPARα-CYP4A pathway is supported by the pattern of expression induced by the positive control, clofibric acid. A decrease in expression of CYP4A was induced by 200 μM clofibric acid, a concentration known to induce CYP4A expression in other cell lines (Ram et al., 1994 and Parmentier et al., 1997), which suggests that the threshold of toxic injury has been surpassed. Therefore, the PPARα-CYP4A pathway in this cell line may be more sensitive and significant CYP4A induction may occur at lower, environmentally relevant concentrations. Further study needs to be conducted to further elucidate the pattern of expression.

In this study, there was no significant difference between cells treated with PFNA and the vehicle control. While a dose-dependent response in the mean expression of CYP4A in cells dosed with PFNA was observed, the range of concentrations that increase CYP4A protein expression above the base expression of untreated cells could be too narrow to accurately detect when stranded cetaceans have been exposed. Although, there may be a concentration between 75

μM and 225μM that induces a significant increase in CYP4A expression from the vehicle control, the range of concentrations may be too small to be detectible as a biomarker. Concentrations of PFNA could either be too low or too high to see a response that is measurably different from base CYP4A expression in cetacean cells for many of the live cetaceans sampled.

Comparisons for PFOS are not justified since an inappropriate vehicle was used. Although PFOS was the only chemical that induced a significant change in CYP4A expression, there was not significant fold change of CYP4A for the lower concentrations. Only cells treated with the highest concentration induced an expression of CYP4A that was greater than the untreated cells. Significant fold expression change was not induced by PFOS, and therefore changes in expression in live animals may not be large enough to see a relationship. These patterns suggest that CYP4A may not be an appropriate biomarker for PFAA exposure due to the sensitivity of the pathway.

PPARα Protein Expression

PPARα Expression with Exposure to PFNA

PFNA exposure induced a dose-dependent response in PPARα expression in exposed cells, Figure 2.18. There was a statistically significant difference between dose concentrations but not between the dose concentrations and the vehicle control, DMSO ($p = 0.0288$). The highest dose, 225 μM, induced a significant increase in expression from the two lowest doses, 1 μM and 25 μM. The mean optical density ratios by increasing dose concentration were (mean = 0.0244 ODR, 0.0247 ODR, 0.107 ODR and 0.479 ODR respectively). The expression of PPARα in cells treated with the highest dose was 19-fold greater than the lowest dose. Additionally, the expression of PPARα dosed with 225 μM PFNA was greater than the positive control, 10 μM

Wy-14,643 (mean = 0.479 ODR and 0.386 ODR respectively). While there was an increase in expression at the highest dose, at the three lower doses the expression of PPARα was lower than the DMSO vehicle control (mean =0.127 ODR). Two outliers were removed from the data set, Table 2.2.

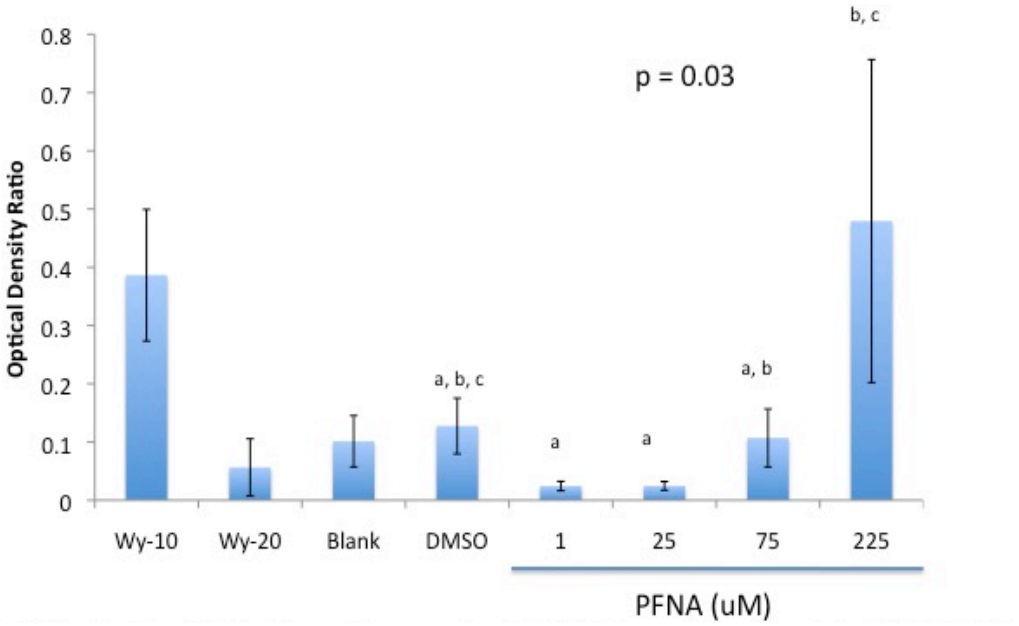

Figure 2.18. PFNA activation of PPARα protein expression
Dolphin kidney cells were treated with Wy-14,643 (10 µM and 20 µM), DMSO (vehicle control), and PFNA at the concentrations indicated. Blank indicates untreated cells. The data show the mean ± SE. The optical density ratio is the ratio of the optical density of the sample to the optical density of an internal control standard of recombinant human PPARα protein from Novus Biologicals. Bars with the same letter indicate values that are not statistically different from each other ($p < 0.05$). n = 4 to 6.

The results of the cell viability assay suggested that toxic injury might occur at the two highest doses of PFNA. This supports a decrease in CYP4A expression in cells treated with 225 µM of PFNA. However, the same pattern was not seen for PPARα expression. PPARα expression was significantly higher at the 225 µM concentration than the two lowest doses. Positive feedback could explain why expression still increased at higher concentrations of PFNA even if the threshold of toxic injury was exceeded. Wan et al., (2012) saw a decrease in

mitochondrial β-oxidation in mice exposed to PFOS. They concluded that the inability to cope with an increase in ω- and peroxisomal β-oxidation could lead to an excess of fatty acids and disturb hepatic lipid homeostasis through positive feedback. Therefore, PPARα may be expressed at greater concentrations in these cells at the highest concentration of PFNA due to an accumulation of fatty acids. The difference in the activation pattern of PPARα and CYP4A could provide information about the mechanism of activation of PFAAs for this pathway, which is still unknown.

PPARα Expression with Exposure to PFDA

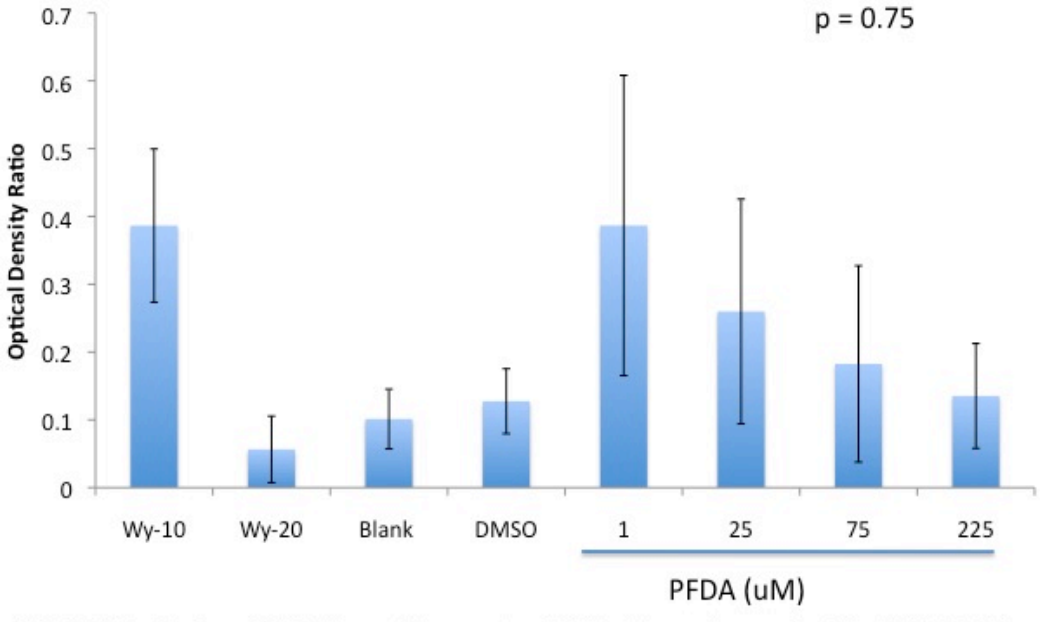

Figure 2.19. PFDA activation of PPARα protein expression
Dolphin kidney cells were treated with Wy-14,643 (10 µM and 20 µM), DMSO (vehicle control), and PFDA at the concentrations indicated. Blank indicates untreated cells. The data show the mean ± SE. The optical density ratio is the ratio of the optical density of the sample to the optical density of an internal control standard of recombinant human PPARα protein from Novus Biologicals. n = 4 to 5.

With increasing concentration of PFDA there was a decrease in PPARα expression, Figure 2.19. The highest expression of PPARα was induced by the lowest concentration of PFDA, 1 µM (mean = 0.387 ODR), and was three-fold greater than the vehicle control, DMSO (mean = 0.101 ODR). All four concentrations induced greater PPARα expression than the vehicle control. PPARα expression was greater for the lowest concentration, 1 µM, (mean = 0.387 ODR) than the lower concentration of Wy-14,643, 10 µM (mean = 0.386 ODR). However, there was no statistical difference between PFDA treated cells and the vehicle control ($p = 0.7515$).

PPARα Expression with Exposure to PFOA

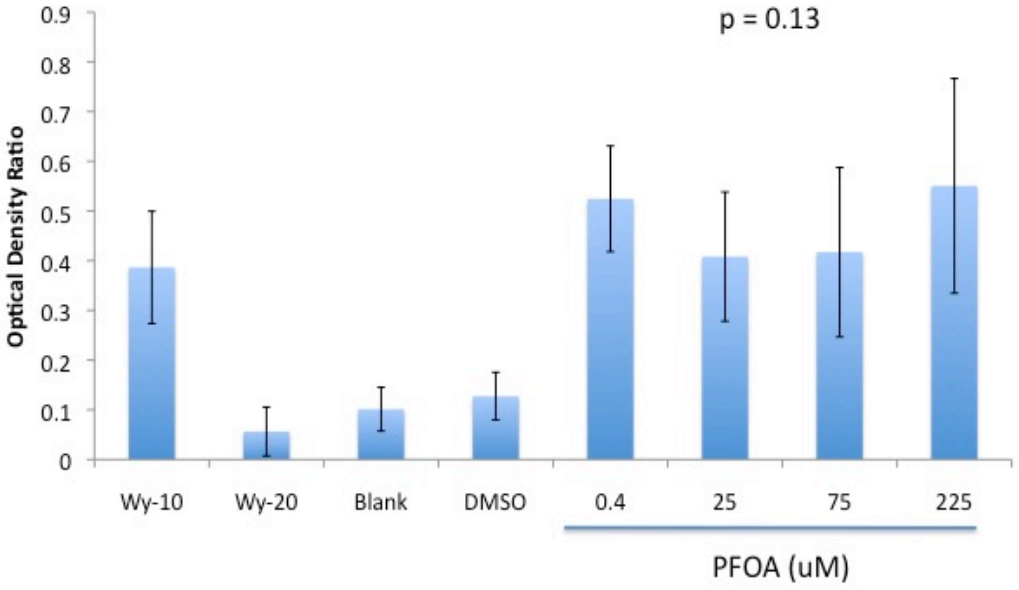

Figure 2.20. PF0A activation of PPARα protein expression
Dolphin kidney cells were treated with Wy-14,643 (10 µM and 20 µM), DMSO (vehicle control), and PFOA at the concentrations indicated. Blank indicates untreated cells. The data show the mean ± SE. The optical density ratio is the ratio of the optical density of the sample to the optical density of an internal control standard of recombinant human PPARα protein from Novus Biologicals. n = 6.

Unlike PFDA and PFNA, a unimodal dose response was not seen in cells exposed to PFOA, Figure 2.20. PPARα expression was greater in the highest and lowest doses of PFOA than the two middle doses. The mean optical density ratios for increasing dose concentration were 0.524 ODR, 0.408 ODR, 0.417 ODR and 0.550 ODR respectively. PPARα expression was greater in all four dose treatments than the greatest expression induced by the positive control 10 µM Wy-14,643 (mean = 0.386 ODR). However, there was no significant difference between PFOA dosed cells and the vehicle control DMSO (p = 0.1289).

PPARα Expression with Exposure to PFOS

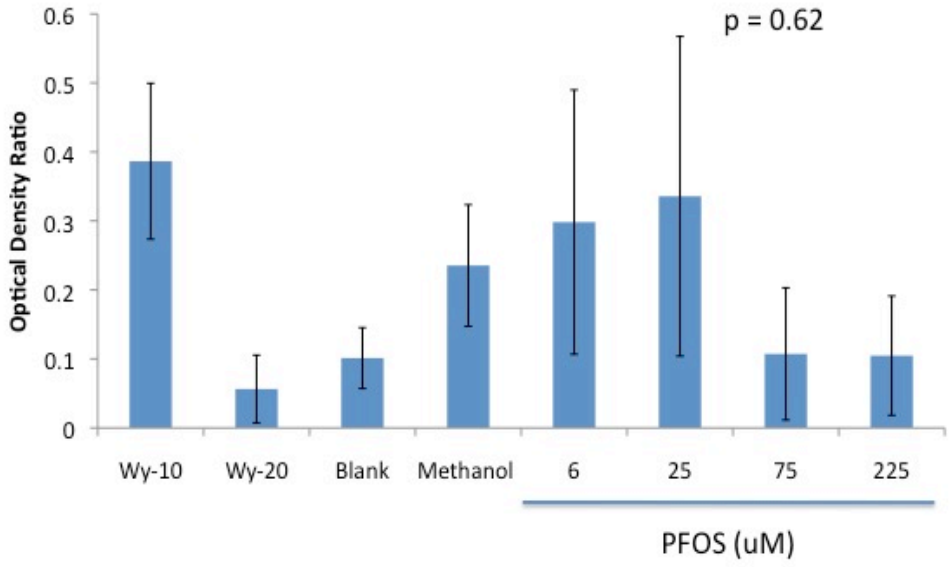

Figure 2.21. PF0S activation of PPARα protein expression
Dolphin kidney cells were treated with Wy-14,643 (10 µM and 20 µM), Methanol (vehicle control), and PFOS at the concentrations indicated. Blank indicates untreated cells. The data show the mean ± SE. The optical density ratio is the ratio of the optical density of the sample to the optical density of an internal control standard of recombinant human PPARα protein from Novus Biologicals. n = 5 to 6.

PPARα expression increased with exposure to the two lowest concentrations, 6 μM and 25 μM of PFOS (mean = 0.298 ODR and 0.336 ODR respectively), Figure 2.21. For the two higher concentrations, 75 μM and 225 μM, PPARα expression decreased to (mean = 0.107 ODR and 0.105 ODR respectively). PPARα expression was greater for all four concentrations of PFOS than the positive control 20 μM Wy-14,643 and untreated cells (mean = 0.564 ODR and 0.101 ODR respectively). However, there was no significant difference between PPARα expression of cells treated with PFOS and the vehicle control ($p = 0.6244$). Two outliers were removed from the data set, Table 2.2.

Relationship Between PFAA Structure and PPARα Expression

The expression of PPARα was hypothesized to be greater with carbon-chain length up to eight carbons (Wolf et al., 2012). When compared across concentrations, PFOA (C-8) induced the highest expression of PPARα, which follows this trend. For both the highest and lowest concentrations of PFOA, the induction of PPARα was higher than any other chemical measured. Comparing relative expression of PPARα induced by PFNA (C-9) and PFDA (C-10) by concentration is difficult, because their expression profiles oppose each other. With increasing concentration of PFDA the expression of PPARα decreases, whereas with the increasing concentration of PFNA the expression of PPARα increases. The highest expression for each chemical is relatively similar. The mean optical density ratio of 1 μM PFDA was 0.387 while the mean optical density ratio of 225 μM PFNA was 0.479.

The response of PPARα to PFNA and PFDA was different than the response seen in other mammals. Wolf et al., (2012) found that the minimum concentration to elicit a significant change in expression for both PFDA and PFNA in COS-1 cells transfected with mouse PPARα

LBD was 5μM. In the same cells transfected with the human LBD > 100 μM PFDA was needed to elicit a significant response while only 5μM of PFNA was needed to elicit a significant response. This was opposite of the pattern seen in these cells were PFDA elicited a greater response at lower concentrations. Additionally, neither PFNA nor PFDA induced a change in expression that was statistically different from the control. To fully understand the relationship between carbon chain length and PPARα expression in these cells more concentration and more chemicals with different chain lengths need to be tested.

The trend of greater expression induced by carboxylates than sulfonates of the same carbon-chain length (Wolf et al., 2012) was observed for PPARα as well as CYP4A. PFOA induced greater expression of PPARα for all concentrations (mean = 0.524 ODR, 0.408 ODR, 0.417 ODR and 0.550 ODR) than the highest expression of PPARα induced by PFOS (mean = 0.336 ODR). Therefore, the trend of higher induction from PFCAs is upheld in these cells for the chemicals tested. However, more chemicals could be tested to see if this trend holds for PFCAs and PFSAs of different carbon-chain lengths.

PPARα as a Biomarker of PFAA Exposure in Cetaceans

Ishibashi et al., (2008) suggested that PPARα could be a viable marker for PFAA exposure in marine mammals; however, the pattern of protein expression in this study did not corroborate their results. This could be a result of differences between mRNA expression and protein expression. Furthermore, it could be a result of using transfected cells that can induce expression of a gene, but are not given additional genes to control the repression of the pathway. Ishibashi et al., (2008) saw significant fold-increase in expression of PPARα mRNA in cells treated with up to 500 μM of PFNA, PFDA, PFOS and PFOA. Our results showed that there was no significant difference ($p < 0.05$) between the vehicle control and PFDA, PFOS, and PFOA

induced expression. PFNA did induce a dose-dependent expression change in PPARα expression, but the fold change at lower concentrations was not significant.

Furthermore, our results indicated that the PPARα-CYP4A pathway in cetacean cells is more sensitive to changes in concentration than other cell lines. With increasing concentration of PFDA and PFOS, protein expression decreased above 25 μM, which could indicate the higher concentrations exceed the threshold of toxic injury. Increased sensitivity of the pathway was supported by the pattern of expression induced by the positive control. PPARα expression decreased at the highest concentration of Wy-14,643, a concentration known to increase expression in other cell lines. The decrease in PPARα expression suggests the threshold of toxic injury was exceeded and this pathway may be more sensitive to lower concentrations than other cell lines.

The lowest concentration of PFOA used, which is a concentration found in exposed animals, may also exceed the threshold of toxic injury. If the threshold of toxic injury is exceeded a clear pattern of expression (a pattern that is not unimodal) may not be seen at higher concentrations. The pattern of expression induced by PFOA was not unimodal. Exceeding the toxic threshold is supported by the results of the cell viability assay, which show a decrease in cell viability with increasing PFOA concentration. Thus, the patterns of expression indicate that PPARα may not be effective as a biomarker in cetaceans for the range of concentrations tested due to the sensitivity of the pathway.

Future Studies

To elucidate the patterns of PPARα and CYP4A induction observed future studies need to be conducted. Positive controls Wy-14,653 and clofibric acid should be tested at a wider

concentration range to further validate the decrease in expression at the higher concentration was due to toxic injury. Additionally, a wider range of concentrations should be tested for each PFAA, to determine if a significant induction of either protein occurs at concentrations not tested. Finally, additionally PFAAs and PFAA mixtures should be tested to further understand the patterns of chain-length and function group on induction of the pathway. While this study provides a baseline for understanding the effects of PFAA exposure in the DK1 cell line, further studies are needed to clarify and expand upon these results.

Conclusions

For the chemicals and range of doses tested, PPARα and CYP4A do not appear to be good biomarkers for cetacean exposure to PFAAs. Kurtz et al., (2019) did find a correlation between PPARα mRNA and CYP4A protein expression in the kidney and ΣPFAA and ΣPFCA concentrations, which suggests that the PPARα-CYP4A pathway may be a more effective biomarker for PFAAs as a whole instead of as individual compounds. Additionally, the PPARα-CYP4A pathway may be a more effective biomarker for lower concentrations not tested, which are concentrations that marine mammals are exposed to in the environment. Of the chemicals tested, Kurtz et al. (2019) also found a correlation between PPARα mRNA expression in the kidney of stranded cetaceans and with PFDA, ΣPFCAs, and ΣPFAAs. However, it is unknown if PPARα protein from live animals would show the same correlation as mRNA or if mRNA and protein expression of PPARα in these cells differ.

While our results do not support the use of the PPARα and CYP4A proteins as biomarkers for PFAA exposure in cetaceans, studies have shown that whole tissue and cultured cells may not be directly comparable, due to the conditions imposed during cell culture (Rosen et

al., 2013). Rosen et al., (2013) saw a difference in gene regulation between whole tissues and culture mouse hepatocytes. Ishibashi et al., (2008) concluded that differences in LOEC values and concentrations seen in wild animals from which the correlations were drawn suggest that the duration of exposure and PFAA mixes could result in the differences between *in vitro and in vivo* systems. Although the *in vitro* and *in vivo* systems may not be directly comparable, this study provides a baseline for understanding how PFAAs affect the PPARα-CYP4A cell pathway in cetaceans.

While the PPARα-CYP4A pathway appears to be too sensitive to concentration changes and does not display the pattern looked for in an effective biomarker of environmental exposure, the disruption of this pathway could still impact the health of cetaceans. Although only two chemicals PFOS and PFNA elicited a significant induction of CYP4A and PPARα respectively, the results suggest that PFAAs still impact the PPARα-CYP4A pathway. Expression of these proteins for some PFAA doses exceeded the expression induced by lower concentrations of the positive controls. While further study is required to fully understand the patterns of protein expression observed here, these results could suggest that induction of this pathway is occurring at lower concentrations than expected, and the concentrations inducing significant expression are environmentally relevant. If this is the case, cetaceans could be experiencing the health consequences of exposure to PFAAs at concentrations much lower than previously expected.

References:

Abbott, B. (2009). Review of the expression of peroxisome proliferator-activated receptors alpha (PPARα), beta (PPARβ), and gamma (PPARγ) in rodent and human development. Reproductive Toxicology, 27, 246-257.

Abbott B. D., Wolf C. J., Das K. P., Zehr R. D., Schmid J. E., Lindstrom A. B., Strynar M. J., & Lau C. (2009). Developmental toxicity of perfluorooctane sulfonate (PFOS) is not dependent on expression of peroxisome proliferator activated receptor-alpha (PPAR alpha) in the mouse. Reproductive Toxicology, 27(3-4), 258-265.

Abbott, B. A., Wolf, C. J., Schmid, J. E., Das, K. P., Zehr, R. D., Helfant, L., Nakayama, S., Lindstrom, A. B., Strynar, M. J., and Lau, C. (2007). Perfluorooctanoic acid-induced developmental toxicity in the mouse is dependent on expression of perioxisome proliferator-activated receptor-alpha. Toxicological Sciences, 98(2), 571-581.

Adams, J., Houde, M., Muir, D., Speakman, T., Bossart, G., & Fair, P. (2008). Land use and the spatial distribution of perfluoroalkyl compounds as measured in the plasma of bottlenose dolphins (Tursiops truncatus). Marine Environmental Research, 66(4), 430-437.

Ahrens, L., Marusczak, N., Rubarth, J., Dommergue, A., Nedjai, R., Ferrari, C. & Ebinghaus, R. (2010). Distribution of perfluoroalkyl compounds and mercury in fish liver from high-mountain lakes in France originating from atmospheric deposition. Environmental Chemistry, 7, 422–428.

Ahrens, L., Siebert, U., & Ebinghaus, R. (2009). Total body burden and tissue distribution of polyfluorinated compounds in harbor seals (Phoca vitulina) from the German Bight. Marine Pollution Bulletin, 58(4), 520-525.

Aldridge, T. C., Tugwood, J. D., & Green, S. (1995). Identification and characterization of DNA elements implicated in the regulation of CYP4A1 transcription. Biochemical Journal, 306(Pt 2), 473.

Allis, J. W., Brown, B. L., Simmons, J. E., Hatch, G. E., McDonald, A., & House, D. E. (1996). Methanol potentiation of carbon tetrachloride hepatotoxicity: The central role of cytochrome P450. Toxicology, 112(2), 131-140.

Anderson, A. (2008). The induction of CYP2B proteins in rodents by phenobarbital-like inducers: what has been discovered and what remains to be learned. Acta Chimica Slovenica, 55(1), 45.

Apelberg, B., Goldman, L., Calafat, A., Herbstman, J., Kuklenyik, Z., Heidler, J., Needham, L., Halden, R., & Witter, F. (2007). Determinants of fetal exposure to polyfluoroalkyl compounds in Baltimore, Maryland. Environmental Science & Technology, 41(11), 3891-3897.

Armitage, J. M., MacLeod, M., & Cousins, I. T. (2009). Comparative assessment of the global fate and transport pathways of long-chain perfluorocarboxylic acids (PFCAs) and perfluorocarboxylates (PFCs) emitted from direct sources. Environmental Science & Technology, 43(15), 5830-5836.

Asakawa, A., Toyoshima, M., Harada, K., Fujimiya, M., Inoue, K., and Koizumi, A. (2008). The ubiquitous environmental pollutant perfluoroctanoic acid inhibits feeding behavior via peroxisome proliferator-activated receptor-alpha. International Journal of Molecular Medicine, Apr. 21 (4), 439-45.

Bars, R. G., Bell, D. R., & Elcombe, C. R. (1993). Induction of cytochrome p450 and peroxisomal enzymes by clofibric acid in vivo and in VITRO. Biochemical Pharmacology, 45(10), 2045-2053.

Berger, J. & Moller, D. (2002). The Mechanisms of Actions of PPARs. Annual Review of Medicine, 53, 409-435.

Betts, K. S. (2007). Perfluoroalkyl acids: what is the evidence telling us?. Environmental Health Perspectives, 115(5), A250.

Bjork, J. A., & Wallace, K. B. (2009). Structure-Activity Relationships and Human Relevance for Perfluoroalkyl Acid–Induced Transcriptional Activation of Peroxisome Proliferation in Liver Cell Cultures. Toxicological Sciences, 111(1), 89-99.

Chauret, N., Gauthier A Fau - Nicoll-Griffith, D. A., & Nicoll-Griffith, D. A. Effect of common organic solvents on in vitro cytochrome P450-mediated metabolic activities in human liver microsomes. (0090-9556 (Print)).

Cheng, X. and Klaasen, C. D. (2008). Perfluorocarboxylic Acids Induce Cytochrome P450 Enzymes in Mouse Liver through Activation of PPAR-α and CAR Transcription Factors. Toxicological Sciences, 106(1), 29.

Conder, J. M., Hoke, R. A., Wolf, W. d., Russell, M. H., & Buck, R. C. (2008). Are PFCAs bioaccumulative? A critical review and comparison with regulatory criteria and persistent lipophilic compounds. Environmental Science & Technology, 42(4), 995-1003.

Corsini, E., Luebke, R. W., Germolec, D. R., & DeWitt, J. C. (2014). Perfluorinated compounds: Emerging POPs with potential immunotoxicity. Toxicology Letters, 230(2), 263-270.

David, R. M., Jones, H. S., Panter, G. H., Winter, M. J., Hutchinson, T. H., & Kevin Chipman, J. (2012). Interference with xenobiotic metabolic activity by the commonly used vehicle solvents dimethylsulfoxide and methanol in zebrafish (Danio rerio) larvae but not Daphnia magna. Chemosphere, 88(8), 912-917.

Devchand, P. R., Keller, H., Peters, J. M., Vazquez, M., Gonzalez, F. J., & Wahli, W. (1996). The PPAR [alpha]-leukotriene B4 pathway to inflammation control. Nature, 384(6604), 39.

Debier, C., Chalon C Fau - Le Boeuf, B. J., Le Boeuf Bj Fau - de Tillesse, T., de Tillesse T Fau - Larondelle, Y., Larondelle Y Fau - Thome, J.-P., & Thome, J. P. (2006). Mobilization of PCBs from blubber to blood in northern elephant seals (Mirounga angustirostris) during the post-weaning fast. Aqua Toxocol, 16;80(2):149-57.

Devchand, P. R., Keller, H., Peters, J. M., Vazquez, M., Gonzalez, F. J., & Wahli, W. (1996). The PPAR [alpha]-leukotriene B4 pathway to inflammation control. Nature, 384(6604), 39.

Dreyer, A., Weinberg, I., Temme, C., & Ebinghaus, R. (2009). Polyfluorinated compounds in the atmosphere of the Atlantic and Southern Oceans: evidence for a global distribution. Environmental Science & Technology, 43(17), 6507-6514.

Fair, P. A., Houde, M., Hulsey, T. C., Bossart, G. D., Adams, J., Balthis, L., et al. (2012). Assessment of perfluorinated compounds (PFCs) in plasma of bottlenose dolphins from two southeast US estuarine areas: relationship with age, sex and geographic locations. Marine Pollution Bulletin, 64(1), 66-74.

Fossi, M. C., Casini, S., Bucalossi, D., & Marsili, L. (2008). First detection of CYP1A1 and CYP2B induction in Mediterranean cetacean skin biopsies and cultured fibroblasts by Western blot analysis. Marine Environmental Research, 66(1), 3-6.

Houde, M., Balmer, B. C., Brandsma, S., Wells, R. S., Rowles, T. K., Solomon, K. R., et al. (2006). Perfluoroalkyl compounds in relation to life-history and reproductive parameters in bottlenose dolphins (Tursiops truncatus) from Sarasota Bay, Florida, USA. Environmental Toxicology and Chemistry, 25(9), 2405-2412.

Houde, M., De Silva, A. O., Muir, D. C., & Letcher, R. J. (2011). Monitoring of perfluorinated compounds in aquatic biota: An updated review: PFCs in aquatic biota. Environmental Science & Technology, 45(19), 7962-7973.

Hu, W., Jones, P. D., Celius, T., & Giesy, J. P. (2005). Identification of genes responsive to PFOS using gene expression profiling. Environmental Toxicology and Pharmacology, 19(1), 57-70.

Intrasuksri, U., Rangwala, S. M., O'Brien, M., Noonan, D. J., & Feller, D. R. (1998). Mechanisms of peroxisome proliferation by perfluorooctanoic acid and endogenous fatty acids. General Pharmacology, 31, 187–197.

Invitrogen. (2017). *Iblot 2^{TM} 2 Dry Bloting System: User Guide.*

Invitrogen. (2016). *Trizol^{TM} Reagent: User Guide.*

Ishibashi, H., Hirano, M., Kim, E.-Y., & Iwata, H. (2019). In Vitro and In Silico Evaluations of Binding Affinities of Perfluoroalkyl Substances to Baikal Seal and Human Peroxisome Proliferator-Activated Receptor α. Environmental Science & Technology, 53(4), 2181-2188.

Ishibashi, H., Iwata, H., Kim, E., Tao, L., Kannan, K., Tanabe, S., Batoev, V. B., & Petrov, E. A. (2008). Contamination and Effects of Perfluorochemicals in Baikal Seal (Pusa sibirica). 2. Molecular Characterization, Expression Level, and Transcriptional Activation of Peroxisome Proliferator-Activated Receptor α. Environmental Science & Technology, 42(7), 2302-2308.

Ishibashi, H., Kim, E., & Iwata H. (2011). Transactivation Potencies of the Baikal Seal (Pusa sibirica) Peroxisome Proliferator-Activated Receptor α by Perfluoroalkyl Carboxylates and Sulfonates: Estimation of PFOA Induction Equivalency Factors. Environmental Science & Technology, 45(7), 3123-3130.

Johnson, A. F., Johnson, A. L., Edson, K. F., Edson, K. Z., Totah, R. F., Totah, R. A., & Rettie A. F., Rettie, A. E., Cytochrome P450 ω-Hydroxylases in Inflammation and Cancer. (1054-3589 (Print)).

Jones, P. D., Hu, W., De Coen, W., Newsted, J. L., & Giesy, J. P. (2003). Binding of perfluorinated fatty acids to serum proteins. Environmental Toxicology and Chemistry, 22(11), 2639-2649.

Kannan, K., Koistinen, J., Beckmen, K., Evans, T., Gorzelany, J. F., Hansen, K. J., Jones, P. D., Helle, E., Nyman, M. & Giesy, J. P. (2001). Accumulation of perfluorooctane sulfonate in marine mammals. Environmental Science & Technology, 35(8), 1593-1598.

Kannan, K., Perrotta, E., & Thomas, N. J. (2006). Association between perfluorinated compounds and pathological conditions in southern sea otters. Environmental Science & Technology, 40(16), 4943-4948.

Kannan, K., Tao, L., Sinclair, E., Pastva, S. D., Jude, D. J., & Giesy, J. P. (2005). Perfluorinated compounds in aquatic organisms at various trophic levels in a Great Lakes food chain. Archives of Environmental Contamination and Toxicology, 48(4), 559-566.

Kelly, B. C., Ikonomou, M. G., Blair, J. D., Surridge, B., Hoover, D., Grace, R., et al. (2009). Perfluoroalkyl contaminants in an Arctic marine food web: trophic magnification and wildlife exposure. Environmental Science & Technology, 43(11), 4037-4043.

Klaunig, J. E., Hocevar, B. A., & Kamendulis, L. M. (2012). Mode of Action analysis of perfluorooctanoic acid (PFOA) tumorigenicity and Human Relevance. Reproductive Toxicology, 33(4), 410-418.

Kudo, N., Suzuki, E., Katakura, M., Ohmori, K., Noshiro, R., & Kawashima, Y. (2001). Comparison of the elimination between perfluorinated fatty acids with different carbon chain length in rats. Chemico-biological Interactions, 134(2), 203-216.

Kurtz, A. E., Reiner, J. L., West, K. L., & Jensen, B. A. (2019). Perfluorinated Alkyl Acids in Hawaiian Cetaceans and Potential Biomarkers of Effect: Peroxisome Proliferator-Activated Receptor Alpha and Cytochrome P450 4A. Environmental Science & Technology, 53(5), 2830-2839.

Lau, C., Anitole, K., Hodes, C., Lai, D., Pfahles-Hutchens, A., & Seed, J. (2007). Perfluoroalkyl Acids: A Review of Monitoring and Toxicological Findings. Toxicological Sciences, 99(2), 366-394.

Lemal, D., M. (2004). Perspective on fluorocarbon chemistry. Journal of Organic Chemistry, 69(1), 1-11.

Li, D., Han, Y., Meng, X., Sun, X., Yu, Q., Li, Y., Wan, L., Huo, Y., & Guo, C. (2010). Effect of regular organic solvents on cytochrome P450-mediated metabolic activities in rat liver microsomes. Drug metabolism and disposition: the biological fate of chemicals, 38 11, 1922-5 .

Lunardi, D., Abelli, L., Panti, C., Marsili, L., Fossi, M. C., & Mancia, A. (2016). Transcriptomic analysis of bottlenose dolphin (Tursiops truncatus) skin biopsies to assess the effects of emerging contaminants. Marine Environmental Research, 114, 74-79.

Maloney, E. & Waxman, D. (1999). trans-Activation of PPARα and PPARγ by structurally diverse environmental chemicals. Toxicology and Applied Pharmocology, 161, 209-218.

Mangelsdorf, D. J. & Evans, R. M. (1995). The RXR heterodimers and orphan receptors. Cell, 83, 841–50.

Meng, P., Deng, S., Du, Z., Wang, B., Huang, J., Wang, Y., . . . Xing, B. (2017). Effect of hydro-oleophobic perfluorocarbon chain on interfacial behavior and mechanism of perfluorooctane sulfonate in oil-water mixture. Scientific Reports, 7, 44694.

Moore, L. B., Maglich, J. M., McKee, D. D., Wisely, B., Willson, T. M., Kliewer, S. A., et al. (2002). Pregnane X receptor (PXR), constitutive androstane receptor (CAR), and benzoate X receptor (BXR) define three pharmacologically distinct classes of nuclear receptors. Molecular Endocrinology, 16(5), 977-986.

Niimi, S., Kim, E. Y., Iwata, H., Watanabe, M. X., Yasunaga, G., Fujise, Y., & Tanabe, S. (2007). Identification and hepatic expression profiles of cytochrome P450 1–4 isozymes in common minke whales (Balaenoptera acutorostrata). Comparative Biochemistry and Physiology Part B: Biochemistry and Molecular Biology, 147(4), 667-681.

Olsen, G. W. D., PhD, Burris, J. M. M., Burlew, M. M. M., & Mandel, J. H. M. (2003).

Epidemiological Assessment of Worker Serum Perfluorooctanesulfonate (PFOS) and Perfluorooctanoate (PFOA) Concentrations and Medical Surveillance Examinations. Journal of Occupational & Environmental Medicine, 45(3), 260-270.

Parmentier, J. H. (1997). Regulation of CYP4A1 and peroxisome proliferator-activated receptor alpha expression by interleukin Ib, interleukhv 6, and dexamethasone in cultured fetal rat hepatocytes. Biochemical Pharmacology, 54(8), 889.

Pineda Torra, I. s., Fruchart, J.-C., Staels, B., Flavell, D. M., & Jamshidi, Y. (2002). Characterization of the Human PPARα Promoter: Identification of a Functional Nuclear Receptor Response Element. Molecular Endocrinology, 16(5), 1013-1028.

Pistocchi, A., & Loos, R. (2009). A map of European emissions and concentrations of PFOS and PFOA. Environmental Science & Technology, 43(24), 9237-9244.

Prevedouros, K., Cousins, I. T., Buck, R. C., & Korzeniowski, S. H. (2006). Sources, fate and transport of perfluorocarboxylates. Environmental Science & Technology, 40(1), 32-44.

Qazi, M.R., Xia, Z., Bogdanska, J., Chang, S.C., Ehresman, D.J., Butenhoff, J.L., Nelson, B.D., DePierre J.W., Abedi-Valugerdi, M., 2009. The atrophy and changes in the cellular compositions of the thymus and spleen observed in mice subjected to short-term exposure to perfluorooctanesulfonate are high-dose phenomena mediated in part by peroxisome proliferator-activated receptor-alpha (PPARalpha). Toxicology, 584 260, 68–76.

Rakhshandehroo, M., Knoch, B., Müller, M., & Kersten, S. (2010). Peroxisome Proliferator-Activated Receptor Alpha Target Genes. PPAR Research, 2010, 20.

Ram, P. A., & Waxman, D. J. (1994). Dehydroepiandrosterone 3β-sulphate is an endogenous activator of the peroxisome-proliferation pathway: induction of cytochrome P-450 4A and acyl-CoA oxidase mRNAs in primary rat hepatocyte culture and inhibitory effects of Ca2+-channel blockers. Biochemical Journal, 301(3), 753.

Rayne, S. & Forest, K. (2009). Perfluoroalkyl sulfonic and carboxylic acids: A critical review of physicochemical properties, levels and patterns in waters and wastewaters, and treatment methods. Journal of Environmental Science and Health, A44(12), 1145-1199.

Ren, H., Vallanat, B., Nelson, D. M., Yeung, L. W. Y., Guruge, K. S., Lam, P. K. S., . . . Corton, J. C. (2009). Evidence for the involvement of xenobiotic-responsive nuclear receptors in transcriptional effects upon perfluoroalkyl acid exposure in diverse species. Reproductive Toxicology, 27(3), 266-277.

Renner, R. (2001). Growing concern over perfluorinated chemicals. Environmental Science & Technology, 35(7), 154A-160A.

Renner, R. (2006). The long and the short of perfluorinated replacements. Environmental Science & Technology, 40(1), 12-13.

Robertson, G., Leclercq, I., & Farrell, G. C. (2001). II. Cytochrome P-450 enzymes and oxidative stress. American Journal of Physiology-Gastrointestinal and Liver Physiology, 281(5), G1135-G1139.

Rosen, M. B., Schmid, J. E., Das, K. P., Wood, C. R., Zehr, R. D., & Lau, C. (2009). Gene expression profiling in the liver and lung of perfluorooctane sulfonate-exposed mouse fetuses: Comparison to changes induced by exposure to perfluorooctanoic acid. Reproductive Toxicology, 27(3), 278-288.

Rosen, M. B., Schmid, J. R., Corton, J. C., Zehr, R. D., Das, K. P., Abbott, B. D., & Lau, C. (2010). Gene Expression Profiling in Wild-Type and PPARα-Null Mice Exposed to Perfluorooctane Sulfonate Reveals PPARα-Independent Effects. PPAR Research, 2010.

Rosen, M. B., Lee, J. S., Ren, H., Vallanat, B., Liu, J., Waalkes, M. P., . . . Corton, J. C. (2008b). Toxicogenomic dissection of the perfluorooctanoic acid transcript profile in mouse liver: Evidence for the involvement of nuclear receptors PPARα and CAR. Toxicological Sciences, 103(1), 46-56.

Rumsby, P. C., McLaughlin, C. L., & Hall, T. (2009). Perfluorooctane sulphonate and perfluorooctanoic acid in drinking and environmental waters. Philosophical Transactions of the Royal Society A: Mathematical, Physical and Engineering Sciences, 367(1904), 4119-4136.

Shaw, S., Berger, M. L., Brenner, D., Tao, L., Wu, Q., & Kannan, K. (2009). Specific accumulation of perfluorochemicals in harbor seals (Phoca vitulina concolor) from the northwest Atlantic. Chemosphere, 74(8), 1037-1043.

Shipley, J., Hurst, C., Tanaka, S., DeRoos, F., Butenhoff, J., Seacat, A., & Waxman, D. (2004). Trans activation of PPARα and induction of PPARα target genes by perfluorooctane-based chemicals. Toxicological Sciences, 80, 151-160.

Simpson, A. E. C. M. (1997). The cytochrome P450 4 (CYP4) family. General Pharmacology: The Vascular System, 28(3), 351-359.

Singh, I. (1997). Biochemistry of peroxisomes in health and disease. Molecular and Cellular Biochemistry, 167(1-2), 1-29.

Sundström, M., Bogdanska, J., Pham, H. V., Athanasios, V., Nobel, S., McAlees, A., . . . Bergman, Å. (2012). Radiosynthesis of perfluorooctanesulfonate (PFOS) and perfluorobutanesulfonate (PFBS), including solubility, partition and adhesion studies. Chemosphere, 87(8), 865-871.

Tao, L., Kannan, K., Kajiwara, N., Costa, M. M., Fillmann, G., Takahashi, S., & Tanabe, S. (2006). Perfluorooctanesulfonate and related fluorochemicals in albatrosses, elephant seals, penguins, and polar skuas from the Southern Ocean. Environmental Science & Technology, 40(24), 7642-7648.

Takacs, M. L., & Abbott, B. D. (2006). Activation of Mouse and Human Peroxisome Proliferator–Activated Receptors (α, β/δ, γ) by Perfluorooctanoic Acid and Perfluorooctane Sulfonate. Toxicological Sciences, 95(1), 108-117.

Tan, F., Jin, Y., Liu, W., Quan, X., Chen, J., & Liang, Z. (2012). Global Liver Proteome Analysis Using iTRAQ Labeling Quantitative Proteomic Technology to Reveal Biomarkers in Mice Exposed to Perfluorooctane Sulfonate (PFOS). Environmental Science & Technology, 46(21), 12170-12177.

Tanneberger, K., Rico-Rico A Fau - Kramer, N. I., Kramer Ni Fau - Busser, F. J. M., Busser Fj Fau - Hermens, J. L. M., Hermens Jl Fau - Schirmer, K., & Schirmer, K. Effects of solvents and dosing procedure on chemical toxicity in cell-based in vitro assays. (0013-936X (Print)).

Timsit, Y. E., & Negishi, M. (2007). CAR and PXR: The xenobiotic-sensing receptors. Steroids, 72(3), 231-246.

Tomy, G. T., Budakowski, W., Halldorson, T., Helm, P. A., Stern, G. A., Friesen, K., . . . Fisk, A. T. (2004). Fluorinated Organic Compounds in an Eastern Arctic Marine Food Web. Environmental Science & Technology, 38(24), 6475-6481.

Trumble, S. J., & Kanatous, S. B. (2012). Fatty Acid use in Diving Mammals: More than Merely Fuel. Frontiers in Physiology, 3, 184.

Vanden Heuvel, J. P., Thompson, J. T., Frame, S. R., & Gillies, P. J. (2006). Differential activation of nuclear receptors by perfluorinated fatty acid analogs and natural fatty acids: A comparison of human, mouse, and rat peroxisome proliferator-activated receptor-α,-β, and-γ, liver X receptor-β, and retinoid X receptor-α. Toxicological Sciences, 92(2), 476-489.

Van de Vijver, K. I., Hoff, P. T., Das, K., Van Dongen, W., Esmans, E. L., Jauniaux, T., Bouquegneau, J. M., Blust, R. & De Coen, W. (2003). Perfluorinated chemicals infiltrate ocean waters: link between exposure levels and stable isotope ratios in marine mammals. Environmental Science & Technology, 37(24), 5545-5550.

Wahli W., Braissant O., Desvergne B. (1995). Peroxisome proliferator activated receptors: transcriptional regulators of adipogenesis, lipid metabolism and more. Chemistry & Biology, 2, 261–66.

Wan, H. T., Zhao, Y. G., Wei, X., Hui, K. Y., Giesy, J. P., & Wong, C. K. C. (2012). PFOS-induced hepatic steatosis, the mechanistic actions on β-oxidation and lipid transport. Biochimica et Biophysica Acta (BBA) - General Subjects, 1820(7), 1092-1101.

Wang, S.-P., Hu, X.-X., Meng, Q.-W., Muhammad, S. A., Chen, R.-R., Li, F., & Li, G.-Q. (2013). The involvement of several enzymes in methanol detoxification in Drosophila melanogaster adults. Comparative Biochemistry and Physiology Part B: Biochemistry and Molecular Biology, 166(1), 7-14.

Waxman, D. J. (1999). P450 gene induction by structurally diverse xenochemicals: Central role of nuclear receptors CAR, PXR, and PPAR. Biochemistry and Biophysics, 369(1), 11-23.

Wolf, C. J., Takacs, M. L., Schmid, J. E., Lau, C., & Abbott, B. D. (2008). Activation of mouse and human peroxisome proliferator− activated receptor alpha by perfluoroalkyl acids of different functional groups and chain lengths. Toxicological Sciences, 106(1), 162-171.

Yang, Q., Xie, Y., Alexson, S., Nelson, B., & De Pierre, J. (2002). Involvement of the peroxisome proliferator-activated receptor alpha in the immunomodulation caused by peroxisome proliferators in mice. Biochemical Pharmacology, 63, 1893-1900.

Yang, Q., Xie, Y., Eriksson, A. M., Nelson, B. D., & DePierre, J. W. (2001). Further evidence for the involvement of inhibition of cell proliferation and development in thymic and splenic atrophy induced by the peroxisome proliferator perfluoroctanoic acid in mice33Abbreviations: PFOA, perfluorooctanoic acid; PP, peroxisome proliferator; FBS, fetal bovine serum; FITC, fluorescein isothiocyanate; and DEHP, di(2-ethylhexyl)phthalate. Biochemical Pharmacology, 62(8), 1133-1140.

Yao, P.-L., Ehresman, D. J., Rae, J. M. C., Chang, S.-C., Frame, S. R., Butenhoff, J. L., . . . Peters, J. M. (2014). Comparative in vivo and in vitro analysis of possible estrogenic effects of perfluorooctanoic acid. Toxicology, 326, 62-73.

Yoshikawa, T. (2002). What is oxidative stress? JMAJ, 45(7), 271.

Young, C. J., Furdui, V. I., Franklin, J., Koerner, R. M., Muir, D. C. G. & Mabury, S. A. (2007). Perfluorinated acids in Arctic snow: New evidence for atmospheric formation. Environmental Science & Technology, 41, 3455−3461.

Zushi, Y., Ye, F., Motegi, M., Nojiri, K., Hosono, S., Suzuki, T., Kosugi, Y., Yaguchi, K. & Masunaga, S. (2011). Spatially detailed survey on pollution by multiple perfluorinated compounds in the Tokyo Bay basin of Japan. Environmental Science & Technology, 45, 2887−2893.

Appendix A:

Assembling the iBlot™ 2 Transfer Stack (Invitrogen, 2017).

Assembling the iBlot™ 2 Transfer Stack

1. Open the lid of the device using the latch. Ensure the blotting surface is clean.

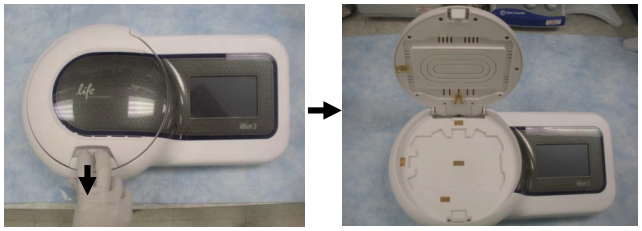

2. Unseal the iBlot™ 2 Transfer Stack.

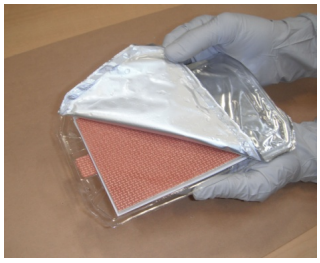

3. Separate the Top Stack and set it to one side of the bench with the transfer gel layer facing up. **Keep the Bottom Stack in the transparent plastic tray.**

   Note: In some instances, the membrane may adhere to the separator. Make sure that the membrane is not stuck to the separator before proceeding to the next step. If the membrane is stuck on the separator, use forceps to remove the membrane and place it on top of the Bottom Stack.

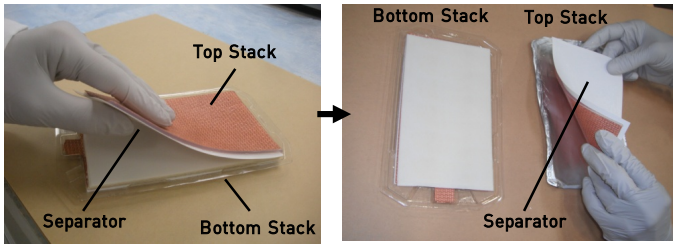

Assembling the iBlot™ 2 Transfer Stack, continued

4. Place the Bottom Stack **with the plastic tray** directly on the blotting surface.

Align the tray in the center of the blotting surface according to the type of iBlot™ 2 Transfer Stack being used.

Do not push trays fully to the top (Mini) or fully to the left (Regular) as this may elevate and twist the tray or interfere with the contacts.

The electrical contacts on the tray should be aligned with the corresponding electrical contacts on the blotting surface of the iBlot™ 2 Gel Transfer Device.

Orientation for iBlot™ 2 **Regular** Transfer Stack

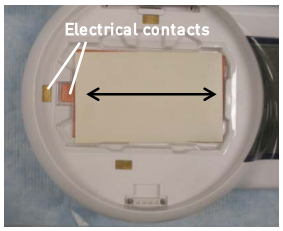

Orientation for iBlot™ 2 **Mini** Transfer Stack

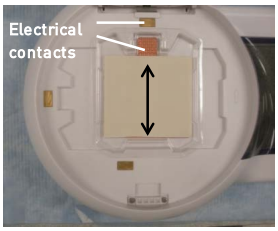

5. Ensure there are no bubbles between the membrane and the transfer stack. Remove any trapped air bubbles using the Blotting Roller.
6. Open the gel cassette and immerse the pre-run gel briefly in deionized water (1–10 seconds) to facilitate easy positioning of the gel on top of the transfer membrane.

   Note: For Novex™ Tris-Glycine Plus gels, rinse in 100 mL of deionized water for 5 minutes to improve transfer of mid to low molecular weight proteins (< 150 kDa).
7. Shake off excess water, and place the pre-run gel on the transfer membrane of the Bottom stack as described:
8. 1 midi gel on an iBlot™ 2 Regular Transfer Stack
9. 2 mini gels (head-to-head) on an iBlot™ 2 Regular Transfer Stack
10. 1 mini gel on an iBlot™ 2 Mini Transfer Stack

Transferring two mini gels

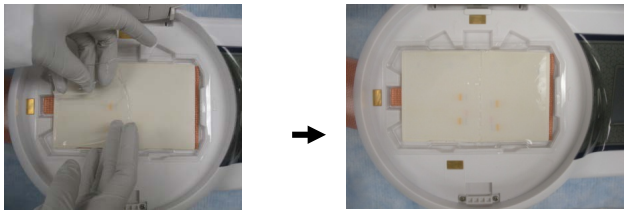

Transferring one mini gel

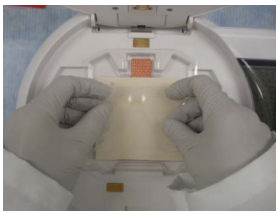

Assembling the iBlot™ 2 Transfer Stack, continued

11. Use the Blotting Roller to remove any air bubbles between the gel and the membrane.
12. Soak the iBlot™ Filter Paper (use the appropriate filter paper for the size of the gel) in a clean container of deionized water. iBlot™ Filter Paper is included with each iBlot™ 2 Transfer Stacks.

    Note: For E-PAGE™ gels, **there is no need** to use a filter paper.

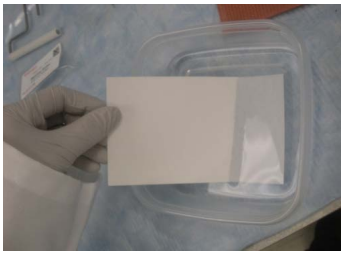

13. Place the presoaked iBlot™ Filter Paper on the pre-run gel. Use the Blotting Roller to remove any air bubbles between the filter paper and gel.

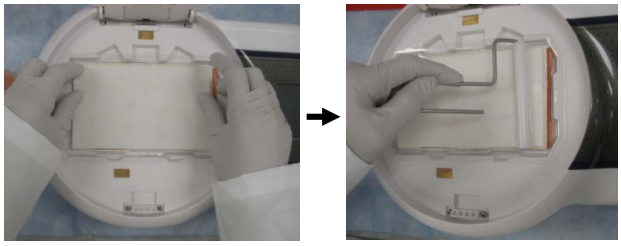

14. Remove and discard the white plastic separator from the Top stack.
15. Take the Top Stack from the bench and place it on top of the presoaked filter paper with the copper electrode facing up (and transfer gel layer facing down). Remove any air-bubbles using the Blotting Roller.

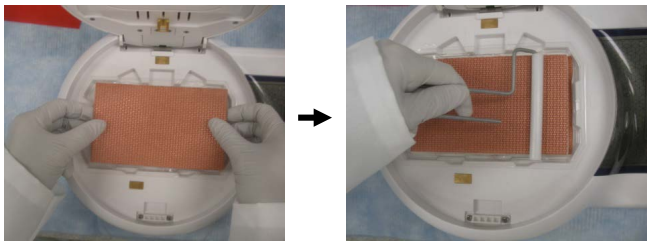

Appendix B:
Trizol™ Reagent User Manual (Invitrogen 2016)

invitrogen USER GUIDE

TRIzol™ Reagent

Catalog Numbers 15596026 and 15596018

Doc. Part No. 15596026.PPS **Pub. No.** MAN0001271 **Rev.** A.0

WARNING! Read the Safety Data Sheets (SDSs) and follow the handling instructions. Wear appropriate protective eyewear, clothing, and gloves. Safety Data Sheets (SDSs) are available from **thermofisher.com/support**.

Product information

Invitrogen™ TRIzol™ Reagent is a ready-to-use reagent, designed to isolate high quality total RNA (as well as DNA and proteins) from cell and tissue samples of human, animal, plant, yeast, or bacterial origin, within one hour. TRIzol™ Reagent is a monophasic solution of phenol, guanidine isothiocyanate, and other proprietary components which facilitate the isolation of a variety of RNA species of large or small molecular size. TRIzol™ Reagent maintains the integrity of the RNA due to highly effective inhibition of RNase activity while disrupting cells and dissolving cell components during sample homogenization. TRIzol™ Reagent allows for simultaneous processing of a large number of samples, and is an improvement to the single-step RNA isolation method developed by Chomcynski and Sacchi (Chomczynski and Sacchi, 1987).

TRIzol™ Reagent allows to perform sequential precipitation of RNA, DNA, and proteins from a single sample (Chomczynski, 1993). After homogenizing the sample with TRIzol™ Reagent, chloroform is added, and the homogenate is allowed to separate into a clear upper aqueous layer (containing RNA), an interphase, and a red lower organic layer (containing the DNA and proteins). RNA is precipitated from the aqueous layer with isopropanol. DNA is precipitated from the interphase/organic layer with ethanol. Protein is precipitated from the phenol-ethanol supernatant by isopropanol precipitation. The precipitated RNA, DNA, or protein is washed to remove impurities, and then resuspended for use in downstream applications.

- Isolated RNA can be used in RT-PCR, Northern Blot analysis, Dot Blot hybridization, poly(A)+ selection, in vitro translation, RNase protection assay, and molecular cloning.
- Isolated DNA can be used in PCR, Restriction Enzyme digestion, and Southern Blots.
- Isolated protein can be used for Western Blots, recovery of some enzymatic activity, and some immunoprecipitation.

TRIzol™ Reagent can also be used with Phasemaker™ Tubes to isolate RNA. Refer to *TRIzol™ Reagent and Phasemaker™ Tubes Complete System User Guide* (MAN0016163) for the full protocol.

Contents and storage

Contents	Cat. No. 15596026 (100 reactions)	Cat. No. 15596018 (200 reactions)	Storage
TRIzol™ Reagent	100 mL	200 mL	15–30°C

Required materials not supplied

Unless otherwise indicated, all materials are available through **thermofisher.com**. MLS: Fisher Scientific (**fisherscientific.com**) or other major laboratory supplier.

Table 1 Materials required for RNA, DNA, and protein isolation

Item	Source
Equipment	
Centrifuge and rotor capable of reaching 12,000 × *g* and 4°C	MLS
Tubes	
Polypropylene microcentrifuge tubes	MLS
Reagents	
Chloroform	MLS

Table 2 Materials required for RNA isolation

Item	Source
Equipment	
Water bath or heat block at 55–60°C	MLS
Reagents	
Isopropanol	MLS
Ethanol, 75%	MLS
RNase-free water of 0.5% SDS	MLS
(Optional) RNase-free glycogen	MLS

Table 3 Materials required for DNA isolation

Item	Source
Reagents	
Ethanol, 100%	MLS
Ethanol, 75%	MLS
0.1 M sodium citrate in 10% ethanol	MLS
8 mM NaOH	MLS
HEPES	MLS

Table 4 Materials required for protein isolation

Item	Source
Equipment	
(Optional) Dialysis membranes	MLS
Reagents	
Isopropanol	MLS
Ethanol, 100%	MLS
0.3 M Guanidine hydrochloride in 95% ethanol	MLS
1% SDS	MLS

For Research Use Only. Not for use in diagnostic procedures.

ThermoFisher SCIENTIFIC

Input sample requirements

IMPORTANT! Perform RNA isolation immediately after sample collection or quick-freeze samples immediately after collection and store at –80°C or in liquid nitrogen until RNA isolation.

Sample type	Starting material per 1 mL of TRIzol™ Reagent
Tissues[1]	50–100 mg of tissue
Cells grown in monolayer	1×10^5–1×10^7 cells grown in monolayer in a 3.5–cm culture dish (10 cm^2)
Cells grown in suspension	5–10 $\times 10^6$ cells from animal, plant, or yeasty origin or 1 $\times 10^7$ cells of bacterial origin

[1] Fresh tissues or tissues stored in RNA*later*™ Stabilization Solution (Cat. No. AM7020).

Procedural guidelines

- Perform all steps at room temperature (20–25°C) unless otherwise noted.
- Use cold TRIzol™ Reagent if the starting material contains high levels of RNase, such as spleen or pancreas samples.
- Use disposable, individually wrapped, sterile plastic ware and sterile, disposable RNase-free pipettes, pipette tips, and tubes.
- Wear disposable gloves while handling reagents and RNA samples to prevent RNase contamination from the surface of the skin; change gloves frequently, particularly as the protocol progresses from crude extracts to more purified materials.
- Always use proper microbiological aseptic techniques when working with RNA.
- Use RNase*Zap*™ RNase Decontamination Solution (Cat. no. AM9780) to remove RNase contamination from work surfaces and non-disposable items such as centrifuges and pipettes used during purification.

Lyse samples and separate phases

1. Lyse and homogenize samples in TRIzol™ Reagent according to your starting material.
   - **Tissues:**

     Add 1 mL of TRIzol™ Reagent per 50–100 mg of tissue to the sample and homogenize using a homogenizer.
   - **Cell grown in monolayer:**
     a. Remove growth media.
     b. Add 0.3–0.4 mL of TRIzol™ Reagent per 1×10^5—10^7 cells directly to the culture dish to lyse the cells.
     c. Pipet the lysate up and down several times to homogenize.
   - **Cells grown in suspension:**
     a. Pellet the cells by centrifugation and discard the supernatant.
     b. Add 0.75 mL of TRIzol™ Reagent per 0.25 mL of sample (5–10×10^6 cells from animal, plant, or yeasty origin or 1×10^7 cells of bacterial origin) to the pellet.

        Note: Do not wash cells before addition of TRIzol™ Reagent to avoid mRNA degradation.
     c. Pipet the lysate up and down several times to homogenize.

   Note: The sample volume should not exceed 10% of the volume of TRIzol™ Reagent used for lysis.

   STOPPING POINT Samples can be stored at 4°C overnight or at –20°C for up to a year.
2. *(Optional)* If samples have a high fat content, centrifuge the lysate for 5 minutes at 12,000 × *g* at 4–10°C, then transfer the clear supernatant to a new tube.
3. Incubate for 5 minutes to permit complete dissociation of the nucleoproteins complex.
4. Add 0.2 mL of chloroform per 1 mL of TRIzol™ Reagent used for lysis, then securely cap the tube.
5. Incubate for 2–3 minutes.
6. Centrifuge the sample for 15 minutes at 12,000 × *g* at 4°C.

   The mixture separates into a lower red phenol-chloroform, and interphase, and a colorless upper aqueous phase.
7. Transfer the aqueous phase containing the RNA to a new tube.
8. Transfer the aqueous phase containing the RNA to a new tube by angling the tube at 45° and pipetting the solution out.

   IMPORTANT! Avoid transferring any of the interphase or organic layer into the pipette when removing the aqueous phase.

Proceed directly to "Isolate RNA" on page 2.

Save the interphase and organic phase if you want to isolate DNA or protein. See "Isolate DNA" on page 3 or "Isolate proteins" on page 4 for detailed procedures. The organic phase can be stored at 4°C overnight.

Isolate RNA

1 Precipitate the RNA

a. *(Optional)* If the starting sample is small (<10^6 cells or <10 mg of tissue), add 5–10 µg of RNase-free glycogen as a carrier to the aqueous phase.

   Note: The glycogen is co-precipitated with the RNA, but does not interfere with subsequent applications.
b. Add 0.5 mL of isopropanol to the aqueous phase, per 1 mL of TRIzol™ Reagent used for lysis.
c. Incubate for 10 minutes.
d. Centrifuge for 10 minutes at 12,000 × *g* at 4°C.

   Total RNA precipitate forms a white gel-like pellet at the bottom of the tube.
e. Discard the supernatant with a micropipettor.

2 Wash the RNA

a. Resuspend the pellet in 1 mL of 75% ethanol per 1 mL of TRIzol™ Reagent used for lysis.

   Note: The RNA can be stored in 75% ethanol for at least 1 year at –20°C, or at least 1 week at 4°C.
b. Vortex the sample briefly, then centrifuge for 5 minutes at 7500 × *g* at 4°C.
c. Discard the supernatant with a micropipettor.
d. Vacuum or air dry the RNA pellet for 5–10 minutes.

   IMPORTANT! Do not dry the pellet by vacuum centrifuge. Do not let the RNA pellet dry, to ensure total solubilization of the RNA. Partially dissolved RNA samples have an $A_{230/280}$ ratio <1.6.

3 **Solubilize the RNA**

a. Resuspend the pellet in 20–50 µL of RNase-free water, 0.1 mM EDTA, or 0.5% SDS solution by pipetting up and down.

IMPORTANT! Do not dissolve the RNA in 0.5% SDS if the RNA is to be used in subsequent enzymatic reactions.

b. Incubate in a water bath or heat block set at 55–60°C for 10–15 minutes.

Proceed to downstream applications, or store the RNA at –70°C.

4 **Determine the RNA yield**

Determine the RNA yield using one of the following methods.

Method	Procedure
Absorbance Absorbance at 260 nm provides total nucleic acid content, while absorbance at 280 nm determines sample purity. Since free nucleotides, RNA, ssDNA, and dsDNS absorb at 260 nm, they all contribute to the total absorbance of the sample.	1. Dilute sample in RNase-free water, then measure absorbance at 260 nm and 280 nm. 2. Calculate the RNA concentration using the formula A260 × dilution × 40 = µg RNA/mL. 3. Calculate the A260/A280 ratio. A ratio of ~2 is considered pure. RNA samples can be quantified by absorbance without prior dilution using the NanoDrop™ Spectophotometer. Refer to the instrument's instructions for more information.
Fluorescence Fluorescence selectively measures intact RNA, but does not measure protein or other contaminant present in the sample	• Quantify RNA yield using the appropriate Qubit™ or Quant-iT™ RNA Assay Kit (Cat. Nos. Q32852, Q10210, Q33140, or Q10213). Refer to the kit's instructions for more information.

Table 5 Typical RNA ($A_{260/280}$ of >1.8) yields from various starting materials

Starting material	Quantity	RNA yield
Epithelial cells	1×10^6 cells	8–15 µg
New tobacco leaf	—	73 µg
Fibroblasts	1×10^6 cells	5–7 µg
Skeletal muscles and brain	1 mg	1–1.5 µg
Placenta	1 mg	1–4 µg
Liver	1 mg	6–10 µg
Kidney	1 mg	3–4 µg

Isolate DNA

Isolate DNA from the interphase and the lower phenol-chloroform phase saved from "Lyse samples and separate phases" on page 2.

1 **Precipitate the DNA**

a. Remove any remaining aqueous phase overlying the interphase.

This is critical for the quality of the isolated DNA.

b. Add 0.3 mL of 100% ethanol per 1 mL of TRIzol™ Reagent used for lysis.

c. Cap the tube, mix by inverting the tube several times.

d. Incubate for 2–3 minutes.

e. Centrifuge for 5 minutes at 2000 × *g* at 4°C to pellet the DNA.

f. Transfer the phenol-ethanol supernatant to a new tube.

The supernatant is used for protein isolation (see "Isolate proteins" on page 40, if needed, and can be stored at –70°C for several months.

2 **Wash the DNA**

a. Resuspend the pellet in 1 mL of 0.1 M sodium citrate in 10% ethanol, pH 8.5, per 1 mL of TRIzol™ Reagent used for lysis.

b. Incubate for 30 minutes, mixing occasionally by gentle inversion.

Note: The DNA can be stored in sodium citrate/ethanol for at least 2 hours.

c. Centrifuge for 5 minutes at 2000 × *g* at 4°C.

d. Discard the supernatant with a micropipettor.

e. Repeat step 2a–step 2d once.

Note: Repeat step 2a–step 2d twice for large DNA pellets (>200 µg).

f. Resuspend the pellet in 1.5–2 mL of 75% ethanol per 1 mL of TRIzol™ Reagent used for lysis.

g. Incubate for 10–20 minutes, mixing occasionally by gentle inversion.

Note: The DNA can be stored in 75% ethanol at several months at 4°C.

h. Centrifuge for 5 minutes at 2000 × *g* at 4°C.

i. Discard the supernatant with a micropipettor.

j. Vacuum or air dry the DNA pellet for 5–10 minutes.

IMPORTANT! Do not dry the pellet by vacuum centrifuge.

3 **Solubilize the DNA**

a. Resuspend the pellet in 0.3–0.6 mL of 8 mM NaOH by pipetting up and down.

Note: We recommend resuspending the DNA is a mild base because isolated DNA does not resuspend well in water or Tris buffer.

b. Centrifuge for 10 minutes at 12,000 × *g* at 4°C to remove insoluble materials.

c. Transfer the supernatant to a new tube, then adjust pH as needed with HEPES.

Proceed to downstream applications, or store the DNA at 4°C overnight. For longer-term storage at –20°C, adjust the pH to 7–8 with HEPES and add 1 mM EDTA.

4 **Determine the DNA yield**

Determine the DNA yield using one of the following methods.

Method	Procedure
Absorbance Absorbance at 260 nm provides total nucleic acid content, while absorbance at 280 nm determines sample purity. Since free nucleotides, RNA, ssDNA, and dsDNS absorb at 260 nm, they all contribute to the total absorbance of the sample.	1. Dilute sample in water or buffer (pH >7.5), then measure absorbance at 260 nm and 280 nm. 2. Calculate the DNA concentration using the formula A260 × dilution × 50 = µg DNA/mL. 3. Calculate the A260/A280 ratio. A ratio of ~1.8 is considered pure. DNA samples can be quantified by absorbance without prior dilution using the NanoDrop™ Spectophotometer. Refer to the instrument's instructions for more information.
Fluorescence Fluorescence selectively measures intact DNA, but does not measure protein or other contaminant present in the sample	• Quantify dsDNA yield using the appropriate Qubit™ or Quant-iT™ ds DNA Assay Kit (Cat. Nos. Q32850, Q32851, Q33120, or Q33130). Refer to the kit's instructions for more information.

Table 6 Typical DNA ($A_{260/280}$ of 1.6–1.8) yields from various starting materials

Starting material	Quantity	DNA yield
Fibroblasts	1 × 10^6 cells	5–7 µg
Cultured cells, mammal	1 × 10^6 cells	5–7 µg
Skeletal muscles and brain	1 mg	2–3 µg
Placenta	1 mg	2–3 µg
Liver	1 mg	3–4 µg
Kidney	1 mg	3–4 µg

Isolate proteins

Isolate the proteins from the phenol-ethanol supernatant saved from "Precipitate the DNA" on page 3 using either "Precipitate the proteins" on page 4 or "Dialyse the proteins" on page 5.

1 **Precipitate the proteins**

a. Add 1.5 mL of isopropanol to the phenol-ethanol supernatant per 1 mL of TRIzol™ Reagent used for lysis.

b. Incubate for 10 minutes.

c. Centrifuge for 10 minutes at 12,000 × *g* at 4°C to pellet the proteins.

d. Discard the supernatant with a micropipettor.

2 **Wash the proteins**

a. Prepare a wash solution consisting of 0.3 M guanidine hydrochloride in 95% ethanol.

b. Resuspend the pellet in 2 mL of wash solution per 1 mL of TRIzol™ Reagent used for lysis.

c. Incubate for 20 minutes.

Note: The proteins can be stored in wash solution for at least 1 month at 4°C or for at least 1 year at –20°C.

d. Centrifuge for 5 minutes at 7500 × *g* at 4°C.

e. Discard the supernatant with a micropipettor.

f. Repeat step 2b–step 2e twice.

g. Add 2 mL of 100% ethanol, then mix by vortexing briefly.

h. Incubate for 20 minutes.

i. Centrifuge for 5 minutes at 7500 × *g* at 4°C.

j. Discard the supernatant with a micropipettor.

k. Air dry the protein pellet for 5–10 minutes.

IMPORTANT! Do not dry the pellet by vacuum centrifuge.

3 **Solubilize the proteins**

a. Resuspend the pellet in 200 µL of 1% SDS by pipetting up and down.

Note: To ensure complete resuspension of the pellet, we recommend that you incubate the sample at 50°C in a water bath or heat block.

b. Centrifuge for 10 minutes at 10,000 × *g* at 4°C to remove insoluble materials.

c. Transfer the supernatant to a new tube.

Proceed directly to downstream applications, or store the sample at –20°C.

4	Determine the protein yield •	Measure protein concentration by Bradford assay. **Note:** SDS concentration mush be <0.1%.

Dialyse the proteins

1. Load the phenol-ethanol supernatant into the dialysis membrane.

   Note: The phenol-ethanol solution can dissolve some types of dialysis membranes (cellulose ester, for example). Test dialysis tubing with the membrane to assess compatibility before starting.
2. Dialyze the sample against 3 changes of 0.1% SDS at 4°C. Make the first change of solution after 16 hours, the second change 4 hours later (at 20 hours), and the final change 2 hours later (at 22 hours).

   Note: A SDS concentration of at least 0.1% is required to resolubilize the proteins from the pellet. If desired, the SDS can be diluted after solubilization.
3. Centrifuge the dialysate for 10 minutes at 10,000 × *g* at 4°C.
4. Transfer the supernatant containing the proteins to a new tube.
5. *(Optional)* Solubilize the pellet by adding 100 µL of 1% SDS and 100 µL of 8 M urea.

Proceed directly to downstream applications, or store the sample at –20°C.

Troubleshooting

Observation	Possible cause	Recommended action
A lower yield than expected is observed	The samples were incompletely homogenized or lysed.	Decrease the amount of starting material.
		Cut tissue samples into smaller pieces and ensure the tissue is completely immersed in TRIzol™ Reagent to achieve total lysis.
	The pellet was incompletely solubilized	Increase the solubilization rate by pipetting the sample repeatedly, and heat the sample to 50–60°C.
The sample is degraded	Samples were not immediately processed or frozen after collection.	Sample must be processed or frozen immediately after collection.
	Sample preparations were stored at the incorrect temperature.	Store RNA samples at –60 to –70°C. Store DNA and protein samples at –20°C.
The RNA or DNA is contaminated	The interphase/organic phase is pipetted up with the aqueous phase.	Do not attempt to draw off the entire aqueous layer after phase separation.
	The aqueous phase is incompletely removed.	Remove remnants of the aqueous phase prior to DNA precipitation.
	The DNA pellet is insufficiently washed with 0.1 M sodium citrate in 10% ethanol	Make sure pellet is washed with 0.1 M sodium citrate in 10% ethanol.
The RNA $A_{260/280}$ ratio is low	Sample was homogenized in an insufficient volume of TRIzol™ Reagent.	Add the appropriate amount of TRIzol™ Reagent for your sample type.
	The organic phase is incompletely removed.	Do not attempt to draw off the entire aqueous layer after phase separation.
The DNA $A_{260/280}$ ratio is low	Phenol was not sufficiently removed from the DNA preparation.	Wash the DNA pellet one additional time in 0.1 M sodium citrate in 10% ethanol.

Limited product warranty

References

Chomczynski, P. 1993. *A reagent for the single-step simultaneous isolation of RNA, DNA and proteins from cell and tissue samples.* BioTechniques *15*, 532-537

Chomczynski, P., and Sacchi, N. 1987 *Single Step Method of RNA Isolation by Acid Guanidinium Thiocyanate-Phenol-Chloroform Extraction.* Anal. Biochem. *162*, 156-159

Hummon, A. B., Lim S. R., Difilippantonio, M. J., and Ried, T. 2007 *Isolation and solubilization of proteins after TRIzol® extraction of RNA and DNA from patient material following prolonged storage.* BioTechniques *42*, 467-472